

This is an Open Access document downloaded from ORCA, Cardiff University's institutional repository: <https://orca.cardiff.ac.uk/id/eprint/100354/>

This is the author's version of a work that was submitted to / accepted for publication.

Citation for final published version:

Hu, Kexiang, Awange, Joseph L., Khandu, Forootan, Ehsan , Goncalves, Rodrigo Mikosz and Fleming, Kevin 2017. Hydrogeological characterisation of groundwater over Brazil using remotely sensed and model products. *Science of the Total Environment* 599-60 , pp. 372-386. 10.1016/j.scitotenv.2017.04.188

Publishers page: <http://dx.doi.org/10.1016/j.scitotenv.2017.04.188>

Please note:

Changes made as a result of publishing processes such as copy-editing, formatting and page numbers may not be reflected in this version. For the definitive version of this publication, please refer to the published source. You are advised to consult the publisher's version if you wish to cite this paper.

This version is being made available in accordance with publisher policies. See <http://orca.cf.ac.uk/policies.html> for usage policies. Copyright and moral rights for publications made available in ORCA are retained by the copyright holders.

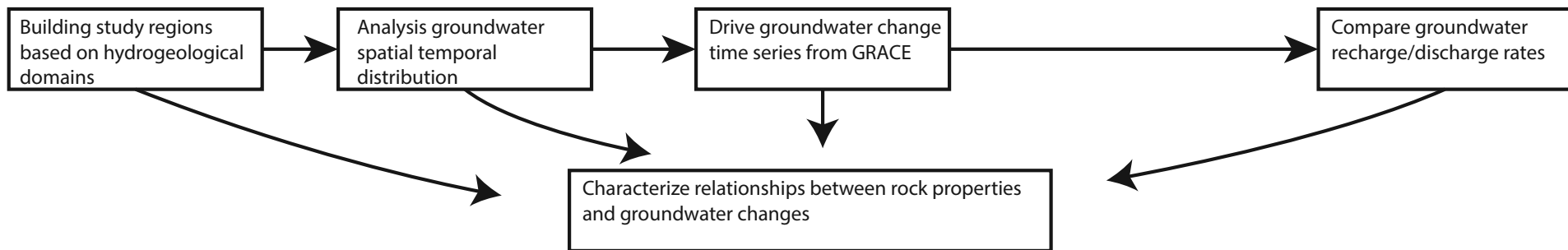
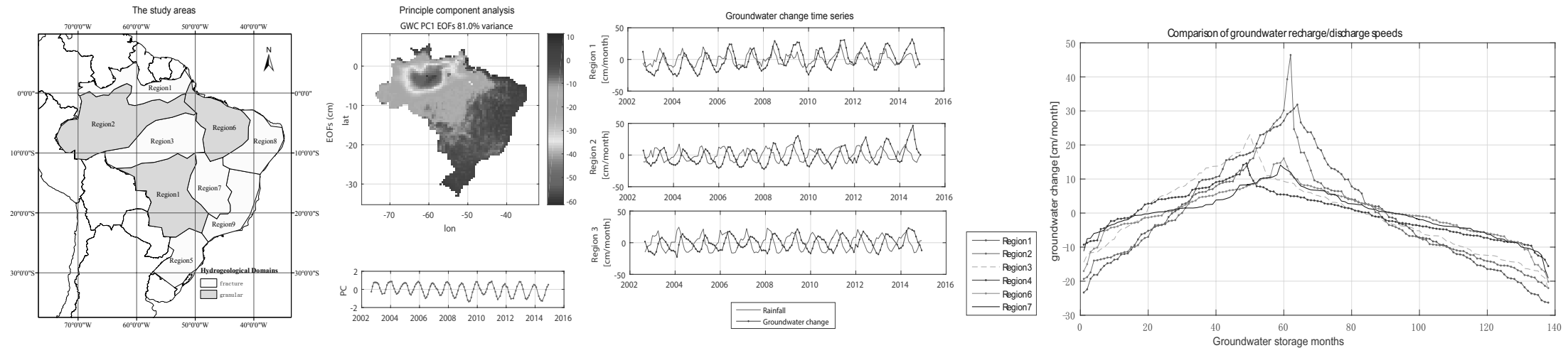


Title: Hydrogeological characterisation of groundwater over Brazil using remotely sensed and model products

Science of The Total Environment, Volumes 599–600, 1 December 2017, Pages 372–386

<http://www.sciencedirect.com/science/article/pii/S0048969717310331>

Cite as: Hu et al. 2017, Science of The Total Environment, Volumes 599-600, Pages 372–386, doi:10.1016/j.scitotenv.2017.04.188



## Highlights

1. Groundwater storage changes estimated from GRACE link geological properties;
2. Rock properties controls groundwater distribution, flow rate and storage capacity;
3. The Amazon area has the largest groundwater change as well as groundwater storage;
4. The dam pattern in Amazon with groundwater  $>0.75$  inflow and  $<0.45$  outflow rates;
5. Wet seasons in in the Amazon regions only occupy about only 36 to 47% of all time.

## Hydrogeological characterisation of groundwater over Brazil

H Kexiang<sup>a</sup>, Joseph L. Awange<sup>a</sup>, Khandu<sup>a</sup>, Ehsan Forootan<sup>b</sup>, Rodrigo Goncalves<sup>c</sup>, Kevin Fleming<sup>d</sup>

<sup>a</sup>*Western Australian Centre for Geodesy and The Institute for Geoscience Research, Curtin University, Perth, Australia*

<sup>b</sup>*School of Earth and Ocean Sciences, Cardiff University, Cardiff, UK*

<sup>c</sup>*Department of Cartographic Engineering, Geodetic Science and Technology of Geoinformation Post Graduation Program, Federal University of Pernambuco (UFPE), Recife, PE, Brazil*

<sup>d</sup>*Centre for Early Warning Systems, GFZ German Research Centre for Geosciences, Potsdam, Germany*

---

### Abstract

1 Groundwater is a valuable source of freshwater across many parts of Brazil, and particularly  
2 during the times of prolonged-droughts. While groundwater storage in Brazil is largely affected  
3 by precipitation variations (e.g., severe droughts), we show that groundwater storage changes  
4 estimated using GRACE time-variable gravity field solutions and hydrological model outputs  
5 (such as GLDAS and WGHM) respond to the spatially varying geological settings across the  
6 country. The impacts of precipitation variability were also taken into account to carefully study  
7 groundwater storage variations under different geological settings in Brazil. The results indicate  
8 that climate variability mainly control groundwater change trends while geological properties  
9 control change rates, spatial distribution, and storage capacity. Granular rocks in the Amazon  
10 and Guarani aquifers are found to influence larger storage capability, higher permeability ( $> 104$   
11  $\text{m/s}$ ) and faster response to rainfall (1–3 months lag) compared to fractured rocks (permeability  
12  $< 107 \text{ m/s}$  and  $> 3$  months lag) found only in Bambui aquifer. Groundwater in the Amazon  
13 region is found to rely not only on precipitation but also on inflow from other regions. Areas  
14 beyond the northern and southern Amazon basin depict a dam-like behaviour, with high inflow  
15 and slow outflow rates (recharge slope  $> 0.75$ , discharge slope  $< 0.45$ ). This is due to two  
16 impermeable rock layer-like walls (permeability  $\approx 108 \text{ m/s}$ ) along the northern and southern  
17 Alter do Chão aquifer that helps retain groundwater. The largest groundwater storage capacity  
18 in Brazil is the Amazon aquifer (with annual amplitudes of  $> 30 \text{ cm}$ ). Amazons groundwater  
19 declined from 2002–2008 due to below normal precipitation (wet seasons lasted for about 36–  
20 47% of the time). The Guarani aquifer and adjacent coastline areas rank second in terms of

21 storage capacity, while the northeast and southeast coastal regions indicate the smallest due to  
22 lack of rainfall (annual average is rainfall  $< 10$  cm).

*Keywords:* Brazil, groundwater changes, hydrogeology, rock properties, GRACE

---

## 23 1. Introduction

24 Groundwater is a very important resource that supports daily life (Cameron, 2012). Globally,  
25 about 97% of the Earth's water exists in the ocean and only 3% on land. Of this amount, 0.61%  
26 consists of groundwater, 0.01% surface water (e.g., lakes and rivers), and the remaining 2.38%  
27 is contained in ice sheets and caps, glaciers, and soil moisture (Harter, 2001). Groundwater,  
28 by contrast to surface water, has the advantage of water storage volume and is usually cleaner  
29 than surface water due to the fact that filtration through the soil helps to purify the incoming  
30 water.

31 In Brazil, a developing country rich in surface water (i.e., the Amazon river), about 16%  
32 of the population rely exclusively on groundwater, which also acts as perennial sources to its  
33 bountiful surface water resources across the country (Hirata and Conicelli, 2012). Although  
34 Brazil is believed to have nearly a fifth of the world's water resources, water shortage problems  
35 still bedevilled most of its states, a situation that is set to continue for a long time in light  
36 of frequent droughts. For example, São Paulo and Rio de Janeiro recently (2014 to 2015)  
37 experienced the worst drought in the last 80 years (Otto et al., 2015; Awange et al., 2016).  
38 Other areas, such as northeastern Brazil and the Amazon River Basin, also suffer from frequent  
39 droughts (e.g., Lemos et al., 2002; Rowland et al., 2015).

40 Numerous studies (e.g., Negri et al., 2004; Vieceli et al., 2015) have tried to understand  
41 water shortage problems and frequent occurrences of droughts by assessing the relationship  
42 between water storage changes (e.g., lakes and rivers) and hydro-meteorological parameters  
43 such as precipitation, temperature and vegetation coverage. However, only a few of these  
44 studies, (e.g., Bahniuk, 2008) managed to link them to subsurface properties such as rock  
45 permeability and layer structure. The spatial distribution of various geological characteristics  
46 and conditions (i.e., rock types and elevation) could be critical factors for understanding the  
47 nature of groundwater storage behaviour across Brazil (e.g., Zagonari, 2010).

48 In fact, from a geological perspective, precipitation controls groundwater changes through  
49 its seasonal and annual variations, providing the main source of water, and when rainfall varies,

50 groundwater follows. Furthermore, i.e., generally speaking, when rain falls to the surface, it  
51 takes time to infiltrate the ground and become groundwater. The speed of fluid moving in rocks  
52 is limited by the size and number of pores, fractures, and permeability of rocks (Farlin et al.,  
53 2013). In addition, rock properties also influence the capacity of storing groundwater in rock  
54 layers due to the limitations in space (pores and fractures) for storing water.

55 To date, most studies that have focused on groundwater in Brazil use isotopic measurements  
56 (e.g., Marimon et al., 2013; Mendonca et al., 2005; Gastmans, 2016), which put radioactive  
57 isotopic atoms into a part of water cycle, i.e., hydrogen in water ( $H_2O$ ), and trace the radiations  
58 in order to detect the groundwater distribution and availability. It is an accurate method for  
59 studying groundwater distribution and availability, but is rather expensive and requires, skilled  
60 experts and long study period (see e.g., Soler and Bonotto, 2015). Usually, such a method is  
61 used to achieve a detailed understanding of the functioning of an aquifer in the area of a well  
62 field, and is therefore difficult to apply over large study area.

63 Also, climatic characteristics (e.g., Broad et al., 2007; Norbre et al., 2016) are usually  
64 used to predict and evaluate drought episodes. However, they rarely link groundwater to  
65 their geological properties and as such, does not offer new information on potential source  
66 of water. Other techniques, such as geothermal methods (e.g., Pimentel and Hamza, 2014),  
67 electromagnetic methods (e.g., Filho et al., 2010) and statistical flow models (e.g., Friedel et  
68 al., 2012) also have been partly applied to infer on the relationship between groundwater and  
69 geological properties (including rock categories) across Brazil, but have been restricted to small  
70 scale characterizations due to the limitation of cost and time.

71 To address these drawbacks, this study utilizes remotely sensed time-variable gravity field  
72 products of the Gravity Recovery and Climate Experiment (GRACE, Tapley et al., 2004) mis-  
73 sion to estimate total water storage (TWS) changes over Brazil (see, e.g., Getirana, 2015; Melo  
74 et al., 2016; Ferreira et al., 2012) . For this, we follow the signal separation approach (e.g., in  
75 Xiao et al., 2015; Cao et al., 2015; Zheng and Chen, 2015; Castellazzi et al., 2016; Forootan  
76 et al., 2014), and remove other forms of water storage (surface water, soil moisture, canopy  
77 water) obtained from models/observations from GRACE TWS. GRACE has already proven  
78 to be a viable technique for monitoring TWS changes (e.g., Han et al., 2009; Abelen et al.,  
79 2015; Sinha et al., 2016). Also, Awange et al. (2014) used GRACE TWS to characterize mega  
80 hydrogeological regimes of Ethiopian, thus showcasing the capability of GRACE products to be

81 linked to geological properties. However, to the best of the authors' knowledge, no study has  
82 attempted to use GRACE products to investigate the relationship between groundwater storage  
83 changes and geological properties in Brazil. Knowledge of groundwater relationships to geolog-  
84 ical characteristics is desirable for understanding aquifer water storage, and recharge/discharge  
85 characteristics. Such knowledge is important for making decisions in water management and  
86 utilization.

87 To complement previous efforts of hydrogeological characterization of groundwater over  
88 Brazil, this study investigates the relationships between groundwater changes and rock prop-  
89 erties by (i) deriving groundwater through subtracting soil moisture, canopy water and surface  
90 water from TWS, (soil moisture and vegetation or canopy water storage can be estimated  
91 from GLDAS (Global Land Data Assimilation System)) (Rodell et al., 2004) products, sur-  
92 face water storage from WGHM (WaterGAP Global Hydrology Model version 2.2a (Döll et al.,  
93 2014; Müller Schmeid et al., 2014)) and various satellite altimetry missions (e.g., Cretaux et  
94 al., 2011)'s products, (ii) employing geological data such as rock layer distribution, elevation,  
95 aquifer types to understand the Brazilian geological conditions, (iii) estimating the impacts  
96 of rainfall on the Brazilian groundwater changes using TRMM (Tropical Rainfall Measuring  
97 Mission) (TMPA, Huffman and Bolvin, 2015) data sets, and (iv) combining (i) and (ii) to  
98 characterise groundwater change behaviours in different rock formations. This is because rock  
99 formations with specific properties could lead to large groundwater storage potential.

100 The study is organised as follows. In Section 2, the hydrogeological characteristics of Brazil-  
101 ian aquifers, which provides the necessary perspective to characterize the GRACE-derived  
102 groundwater changes is presented. Section 3 then provides the data and analysis methods  
103 used in the study while the results are discussed in Section 4, with Section 5 concluding the  
104 study.

## 105 **2. Hydrogeological characteristics of Brazilian aquifers**

### 106 *2.1. Study area*

107 The whole of Brazil is divided into 9 study regions based on fractured and granular rock  
108 formations (Figure 1a). It can be seen that most of the aquifer systems in Brazil are located  
109 within granular rock formations (Figure 1b). From Figure 1c, in North Brazil, the three main

110 aquifer systems (Solimões, Içá and Alter do Chão; Figure 1b) combine to form the Amazon  
 111 aquifer (region 2). Region 4 in the Central-West (upper Paraná basin) consist of the Pantanal,  
 112 Aquidauana and Bauru-Caiuá aquifers, which belong to granular rock formations. Only the  
 113 Serra Geral and Bambuí aquifers in regions 4, 5 and 7 are located in fractured rocks. In  
 114 addition, there are no aquifers located in regions 1 and 3 in the northern and southern sides of  
 115 the Amazon aquifer, respectively, and regions 8 and 9 in the coastal areas of northeastern and  
 116 southeastern Brazil, respectively. Some information on the 9 study regions are summarised in  
 117 Table 1.

Table 1: Some fundamental information about the 9 study regions of Brazil (data source: CPRM, 2014; Ricardo and Bruno, 2011). Note\*: The rock type for each region only represents the first rock layer under the surface.

Region	Rock type*	Aquifer	Groundwater flow direction
1	Fractured	None	North to south
2	Granular	Alter do Chão, Içá and Solimões	West to east
3	Fractured	None	
4	Granular	Bauru-Caiuá, Serra Geral, Botucatu & Piramboia, Pantanal	East to west
5	Fractured	Serra Geral and Botucatu &Piramboia	Northeast to southwest
6	Granular	Itapecuru, Piauí	South to north
7	Fractured	Urucuia and Bambuí	South to north
8	Fractured	None	West to east
9	Fractured	None	West to east

## 118 2.2. Geological properties linked to groundwater

119 Groundwater exists beneath the Earth's surface stored in rock pore spaces and fractures  
 120 (Nelson, 2015). Although precipitation is the main factor that controls the replenishment of  
 121 groundwater, and hence its changes, it is also strongly influenced by rock properties in different  
 122 areas. In Brazil, groundwater is stored in two types of rocks, granular and fractured rocks  
 123 (Figure 1a). The basic difference between these two types of rocks is the way in which water



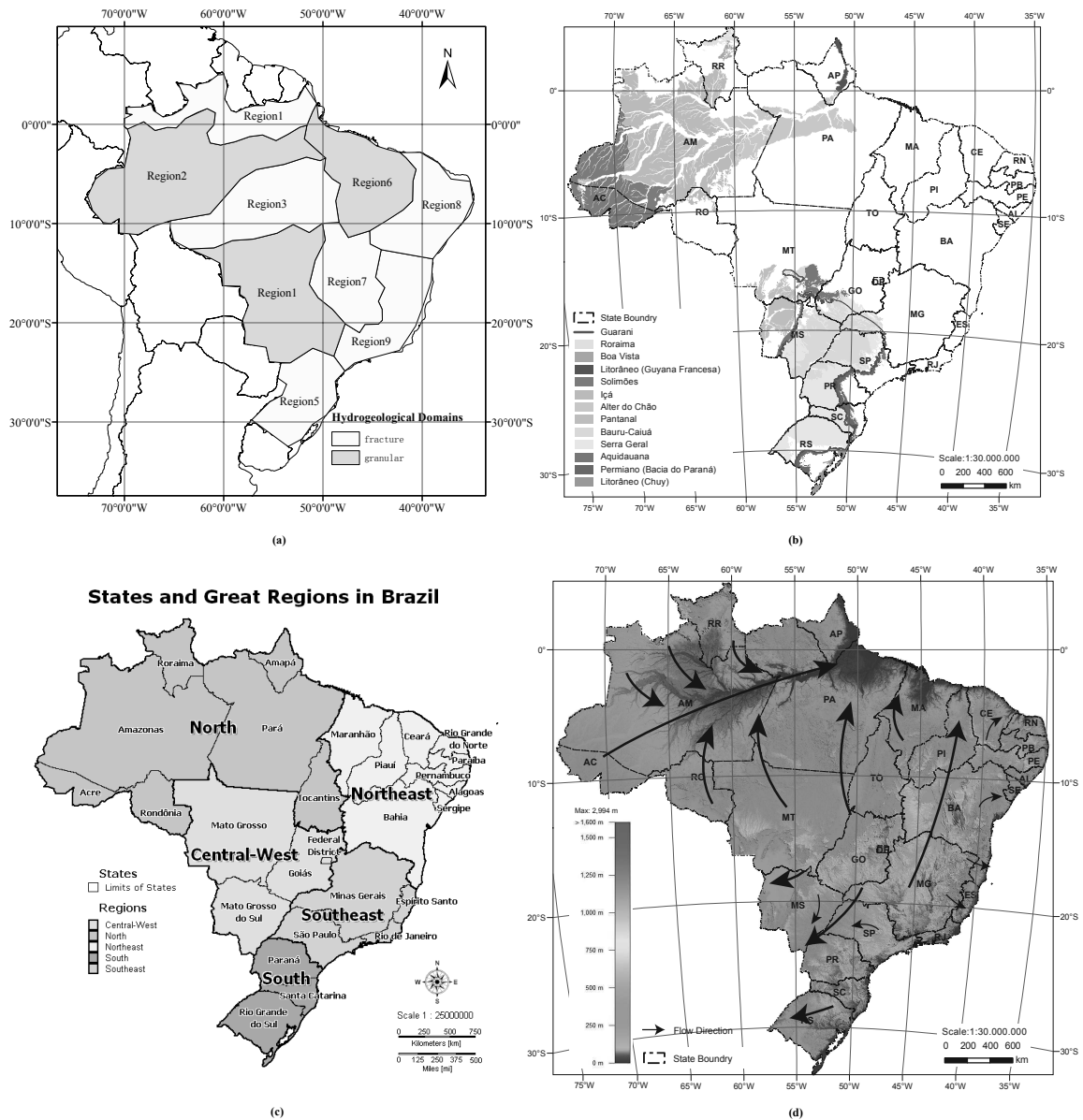


Figure 1: (a) The study areas, (b) the main aquifer systems in Brazil, (c) states and great regions in Brazil, and (d) elevation and general groundwater/surface water flow direction map over Brazil (data source: modified from CPRM, 2014)

124 is stored. Fractured rocks store water in gaps while the granular rocks store water in pore  
 125 spaces (CPRM, 2014; Ricardo and Bruno, 2011). Granular rocks in Brazil mainly include sand,

126 clay, silt, sandstone and conglomerate, and partly contain limestone and dolomite (CPRM,  
127 2014; Ricardo and Bruno, 2011). Fractured rocks mainly consist of basalt, diabase, and mixed  
128 rocks (mixed with granitoid, volcanic and metamorphic rocks). There are also some areas  
129 (i.e, Bambuí aquifer) covered by karst, which is a very special topography that is made up of  
130 creviced rocks with extremely well developed fractures. To understand the GRACE-derived  
131 groundwater behavior in Brazil, the following properties are defined:

132 (i) ‘Porosity’ refers to voids within a rock, and directly determines groundwater storage  
133 capacity. Loose, incompact rocks will have more pore spaces than consolidated rocks. Some  
134 rocks, such as igneous and metamorphic, may have no pore spaces, but could have open spaces  
135 due to fractures. In general, rocks with pore spaces are usually granular, which are permeable  
136 (water can directly pass through) and provide more stable conditions (higher porosity) for  
137 water transport compared to fractured rocks. Fractured rocks are impermeable, that is, water  
138 cannot directly pass through, but only flows via the fractures. Due to the fact that fractures are  
139 not usually distributed homogeneously like pore spaces in rocks, some regions have continuous,  
140 perforated fractures, while others do not. Thus, granular rocks provide more desirable properties  
141 for the storage of groundwater than fractured rocks.

142 (ii) ‘Permeability’ is another important concept, which refers to groundwater flow rates  
143 inside the rocks. Nelson (2015) pointed out that an aquifer is a large body of permeable ma-  
144 terial where groundwater can easily move through via pore space or fractures. According to  
145 different permeability levels, different rock formations are divided into aquifers (high perme-  
146 ability), aquitards (low permeability) and non-aquifers (almost zero permeability). The higher  
147 permeability of a rock formation not only represents a larger potential capacity for storage of  
148 groundwater (more pore space or fractures to store water), but also means a weaker ability to  
149 hold groundwater, i.e., groundwater flows in and out quickly.

150 (iii) ‘Elevation’. Groundwater table level variation usually follow the trend in terrain fluc-  
151 tuation, i.e., high elevation areas usually have higher levels of groundwater table than lower  
152 elevation areas (Charles and William, 2001). Furthermore, groundwater flow directions follow  
153 the principle of hydraulic gradient (i.e., flow from high gradients to low gradients) (Freeze and  
154 Witherspoon, 1967). Figure 1d summarises the surface/groundwater flow directions over Brazil  
155 based on elevation, which can be categorised into three main parts: the north (Amazon), the  
156 centre-west and south parts (Paraná), and the northeastern and southeastern coastal areas of

157 Brazil. First, the centre line of groundwater flow direction in the northern part follows the  
158 Amazon River, which is from west to east. The groundwater flow directions of the areas north  
159 and south of the Amazon basin both point towards the Amazon River. Second, the elevation  
160 distribution of the Paraná basin is high to low from the northeast to the southwest, hence, the  
161 groundwater flow direction. As for the coastal areas, most are split from inland by the Pico da  
162 Bandeira mountain. Groundwater then flows into the Atlantic Ocean from west to east.

### 163 *2.3. Aquifer identification*

164 Groundwater changes are usually associated with multiple rock layers and aquifer types,  
165 which may represent different rock formations and their properties. This makes it challenging  
166 to relate groundwater changes to a single rock formation. It is therefore necessary to identify the  
167 rock formation(s) and aquifer(s) (together with their properties) that contribute to groundwater  
168 changes in Brazil.

169 Aquifers can be of two types, generally, (i) unconfined, where the water table is exposed to  
170 the Earth's atmosphere through the unsaturated zone and (ii) confined, where it is completely  
171 filled with water and separated from the surface by an overlying aquitard or almost impermeable  
172 rock layer. Theoretically, due to the fact that groundwater in an unconfined aquifer can be  
173 quickly replenished by rainfall (direct recharge mechanism), the water table varies from season  
174 to season. By contrast, the groundwater changes in confined aquifers are relatively small and  
175 do not suffer from seasonal changes since the aquifer can only be recharged via slow infiltration  
176 (indirect recharge mechanism) from the overlying aquitards or almost impermeable rock layers.  
177 Therefore, groundwater storage changes derived from GRACE will largely represent changes in  
178 unconfined aquifers.

179 Figure 1b shows the main aquifer systems over Brazil, which are defined only by the first rock  
180 formation under the Earth's surface. According to Alisson (2014), the largest two groundwater  
181 reservoirs in Brazil are the Amazon and Guarani aquifers, which represent more than 80% of  
182 the total water storage in the Amazon and Paraná basins.

183 The Amazon aquifer, located in northern Brazil, consists of the Solimões, Içá and Alter do  
184 Chão aquifer systems from west to east (Figure 2a). Figures 2c and 2d give a cross section of  
185 the Solimões to Içá (A-A') and Alter do Chão aquifer systems (B-B'), respectively. It is clear  
186 that the Içá is the thinnest unconfined aquifer system above Solimões and Alter do Chão. The

187 semi-unconfined Solimões is half exposed to the west, while the other half is under the Içá. As  
188 for the biggest semi-unconfined Alter do Chão aquifer system, one third of its outcropping is in  
189 the Amazon basin and the rest of it is under the Solimões and Içá aquifer systems. With regards  
190 to the groundwater volume capacity, the groundwater storage of the Içá and Solimões (7,200  
191 km<sup>3</sup>) are only 22% of the Alter do Chão aquifer system (33,000 km<sup>3</sup>). Therefore, the Alter do  
192 Chão is the main aquifer system that contributes to groundwater changes in the Amazon basin.  
193 The rock formation characteristics and hydraulic features of the Alter do Chão, Solimões and  
194 Içá are presented in Table 2.

195 Compared to the Amazon aquifer, the geological conditions of the Guarani (2b) are much  
196 more complex due to the fact that it is located over areas ranging from mountains to basins.  
197 Figure 2b only gives a very general overview of the horizontal distribution of the components  
198 of the Guarani aquifer system and shows the vertical structure of three aquifer systems, the  
199 Bauru (the 1st rock formation), the Serra Geral (the 2nd rock formation) and the Botucatu and  
200 Piramboia (the 3<sup>rd</sup> rock formation). More detailed information can be found in, e.g., CPRM  
201 (2014). Following Ondra (2002), the formation characteristics and hydraulic features of the  
202 Bauru, Serra Geral, Botucatu and Piramboia are presented in Table 2. From a thickness point  
203 of view, the Serra Geral varies a great deal, ranging from 20 m to 1,200 m from one area to  
204 another. The Botucatu and Piramboia have an average thickness of 500 to 600 m, while the  
205 Bauru is only about 200 m in thickness on average. Obviously, the Botucatu and Piramboia  
206 rock formations make up the biggest part of groundwater volume with the highest permeability.  
207 The Serra Geral layer also consists of a large part of the Guarani aquifer system, however, the  
208 fractured rocks do not have so much space to store water. Hence, the Botucatu and Piramboia  
209 mainly control groundwater changes in the Guarani aquifer.

#### 210 *2.4. 'Dam' and 'basin' reservoirs patterns*

211 Sometimes, for an area with a specific elevation and rock layer distribution, a new structure  
212 will be formed, which exerts a major influence on groundwater storage and change. 'dam' and  
213 'basin' reservoirs patterns are two such structures established to influence groundwater over  
214 Brazil in this study.

215 First, there are two impermeable rock layers like 'walls' standing at the northern and south-  
216 ern sides of the edges of the Alter do Chão (see Figure 2a), which consist of basalt, diabase, and

Table 2: Rock type descriptions of the Amazon and Guarani aquifers, together with their hydraulic features (data source: CPRM, 2014; Ondra, 2002; Eliene et al., 2013).

Stratigraphic Formation	Aquifer type	Rock type	Rock component	Permeability (m/s)	Water storage identification
Amazon aquifer system					
Içá	unconfined	granular	fine to medium sandstones and siltstones	$1 \times 10^{-5}$ to $1 \times 10^{-6}$	small
Solimões	semi-unconfined	granular	greenish argillaceous sandstones	$5 \times 10^{-5}$ to $1 \times 10^{-6}$	small
Alter do Chão	semi-unconfined	granular	coarse and friable sandstones	$2.1 \times 10^{-4}$ to $5.0 \times 10^{-5}$	large
Guarani aquifer system					
Bauru	unconfined	granular	sandstone with quartz dominant and carbonatic	$1 \times 10^{-5}$ to $1 \times 10^{-6}$	small
Serra Geral	semi-unconfined	fractured	sandstone with quartz dominant and carbonatic	$5 \times 10^{-5}$ to $5 \times 10^{-7}$	small
Botucatu & Piramboia	semi-unconfined	granular	aeolian sandstone with quartz plus feldspars	$1.5 \times 10^{-4}$	large

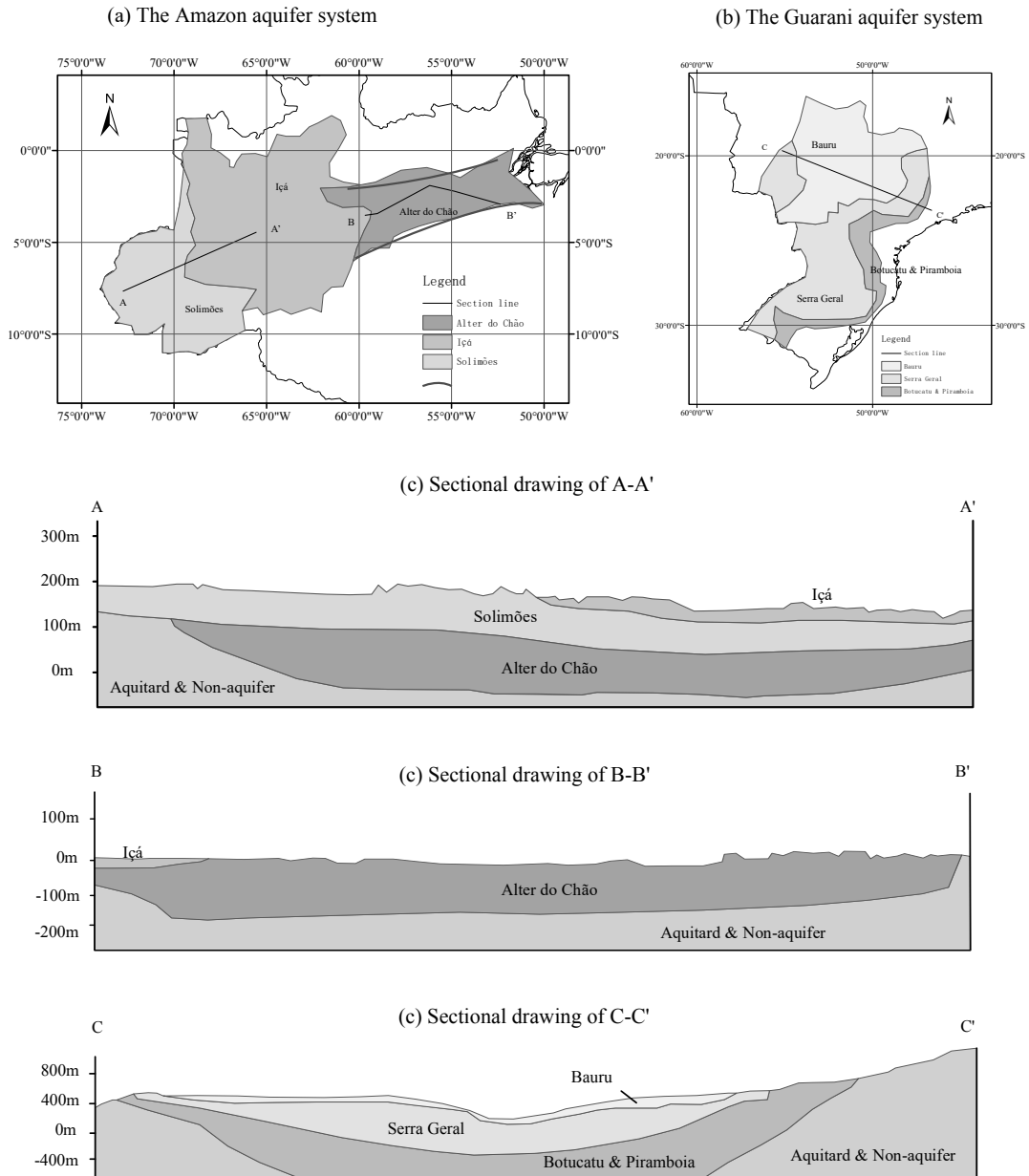


Figure 2: (a) The Amazon aquifer system. (b) The Guarani aquifer system. (c) Sectional drawing of the Solimões, Içá. (d) Sectional drawing of the Alter do Chão. (e) Sectional drawing of the Guarani aquifer system (data source: modified from CPRM, 2014)

217 mixed rocks. Detailed information can be found in the geology map of CPRM (2014). From

218 Figure 1d, one can see that groundwater and surface water are converging from areas beyond  
219 the north and south of the Amazon basin. However, when groundwater meets the northern and  
220 southern edges of the Alter do Chão, they hit the ‘walls’. These two impermeable rock layers  
221 with permeability less than  $1 \times 10^{-8}$  m/s slows the groundwater flow into the Amazon basin  
222 to a large extent. Hence, the groundwater gathers near these two edges like dams retaining  
223 water. Thus, a large volume of groundwater storage can be expected in areas to the northern  
224 and southern sides of the Amazon basin if there is enough rainfall as a source of groundwater.

225 Second, the Guarani aquifer system is a very good example of the ‘basin’ reservoir pat-  
226 tern. Figure 2e shows the structures of the two main Guarani aquifer systems in the west-east  
227 direction, the Serra Geral, and the Botucatu and Piramboia, which lie in a ‘U’ shape. The  
228 groundwater flow direction in the Guarani aquifer system is therefore from two sides towards  
229 the middle, and the groundwater changes depend to a large extent on the size of the direct  
230 recharge area, which is very small at the two sides of the Guarani aquifer (outcrops of Serra  
231 Geral, Botucatu and Piramboia, see Figure 2b). However, due to the Paraguay Paraná plain  
232 being located to the east of the Guarani aquifer, the run-off speed of groundwater from the  
233 northwestern to southeastern direction will be slow, which making it possible for the Guarani  
234 aquifer with small direct recharge areas to gather groundwater slowly if there is enough rain-  
235 fall as a source of groundwater. Stable groundwater storage and changes (both spatially and  
236 temporally), therefore, will be expected in the Guarani aquifer.

### 237 *2.5. Indicators of large potential groundwater storage capacity*

238 The contents of the hydrogeological characteristics above and the expected relationships  
239 between rock properties and groundwater behavior are summarised in Table 3. They provide  
240 the basic characteristics for comparison and evaluation of the results derived from remotely  
241 sensed GRACE and TRMM products, together with the WGHM and GLDAS model outputs.

## 242 **3. Data and methodology**

### 243 *3.1. Data*

244 Various satellite-based and hydrological model data sets are employed in this study to in-  
245 vestigate the relationship between changes and rock properties. The data sets are summarised  
246 in Table 4

Table 3: Geological characteristics linked to groundwater changes.

Geological characteristics	Relationships with respect to groundwater changes
Granular rock type	Stable transmitting conditions and large storage potential.
High permeability	Large storage potential, but weak retaining capability.
Unconfined aquifer	Large storage potential and direct recharge mechanism.
‘Dam’ reservoir	High groundwater increasing speed, but slow outflow speed.
‘Basin’ reservoir	Storage and changes depend on the size of the recharge areas.

247 *3.1.1. GRACE*

248 The Gravity Recovery and Climate Experiment (GRACE) satellites were designed and  
 249 launched by the National Aeronautics and Space Administration (NASA) and the German  
 250 Space Agency (DLR) to detect changes in the Earth’s gravity field. GRACE consists of twin  
 251 satellites moving at low altitude orbits of 300 to 500 km (Tapley et al., 2004) with an ability to  
 252 detect water changes of about 0.9 mm (Andersen et al., 2005). For an accuracy of millimeters  
 253 level in TWS derived from GRACE to be achieved, the basin sizes should be greater than its  
 254 spatial resolution is more than 200,000 km<sup>2</sup> (see, e.g., Zhiyong et al., 2015; Tapley et al., 2004).

255 For this study, GRACE products (LR05: Release-05 GRACE Level-2 product) are ob-  
 256 tained from the CSR (University of Texas Center for Space Research) centre ([http://www.csr.  
 257 utexas.edu/grace/RL05.html](http://www.csr.utexas.edu/grace/RL05.html)). The data are processed based on the approaches of Wahr et  
 258 al. (1998); Swenson and Wahr (2006); Jekeli (1981) using a Gaussian filter of radius 300 km  
 259 (Jekeli, 1981) to remove the noise. GRACE products provides a map of the Earth’s gravity  
 260 changes, which can be converted to water equivalent height (TWS). For a consistent comparison  
 261 with the gridded GLDAS data sets as well as reducing the leakage error by the filters, GRACE  
 262 data is converted from 1° × 1° to 0.5° × 0.5° resolution and multiplied by a gridded scale factor  
 263 derived from the GLDAS TWS following Landerer and Swenson (2012).



264 *3.1.2. TRMM*

265 The Tropical Rainfall Measurement Mission (TRMM, Kummerow et al., 1998) is a collab-  
266 orative effort between NASA and the Japanese Aerospace Exploration Agency (JAXA). The  
267 satellite was launched in 1997 into a near circular orbit of approximately 350 km with a period  
268 of 92.5 minutes. Here, we use the monthly gridded product TRMM 3B43 that are generated  
269 by the TRMM Multi-satellite Precipitation Analysis (TMPA, Huffman and Bolvin, 2015). The  
270 monthly TRMM 3B43 products, hereafter as TRMM, are provided at a spatial resolution of  
271  $0.25^\circ \times 0.25^\circ$  and can be obtained from [https://pmm.nasa.gov/data-access/downloads/](https://pmm.nasa.gov/data-access/downloads/trmm)  
272 [trmm](https://pmm.nasa.gov/data-access/downloads/trmm)). To be consistent with GRACE-derived TWS, the TRMM derived values are converted  
273 to  $0.5^\circ \times 0.5^\circ$ .

274 *3.1.3. GLDAS*

275 The Global Land Data Assimilation (GLDAS) was developed by NASA Goddard Space  
276 Flight (GSFC), the National Oceanic Atmospheric Administration (NOAA) and the National  
277 Centre for Environmental Prediction (NCEP) (Rodell et al., 2004; Hualan and Hiroko, 2016;  
278 Zheng and Chen, 2015). It provides land surface fluxes with a 3 hours and monthly temporal  
279 resolution, and two spatial resolutions,  $1^\circ$  and  $0.25^\circ$ . There are four types of Land Surface  
280 Models (LSM) that GLDAS concentrates on; i.e., MOSAIC, NOAH, CLM and VIC. In this  
281 study, NOAH LSM data (obtained from <http://disc.sci.gsfc.nasa.gov/uui/datasets>)  
282 with a spatial resolution of  $0.25^\circ \times 0.25^\circ$  are applied to derive soil moisture and canopy water  
283 variations. To be consistent with GRACE, GLDAS data sets are processed in the same manner  
284 and converted to  $0.5^\circ \times 0.5^\circ$  resolution using the same scale factor as with GRACE.

285 *3.1.4. WGHM*

286 The WaterGAP Global Hydrology Model (WGHM) simulates the continental water cycle  
287 using conceptual formulations for the most important hydrological processes (Werth and Gunt-  
288 ner, 2010; Döll et al., 2014). In this study, WGHM provides data sets of global TWS, soil  
289 moisture, canopy, reservoirs, lakes and groundwater storage, with a spatial resolution of  $0.5^\circ$   
290  $\times 0.5^\circ$ , which are used to evaluate the groundwater changes derived from GRACE. Besides,  
291 WGHM groundwater model variants IRR\_70\_S (deficit irrigation at 70% of optimal irrigation  
292 with groundwater recharge from surface bodies) and NOUSE\_S (no water use at all assumed  
293 with groundwater recharge from surface bodies) are used to evaluate the human consumption

294 of groundwater.

### 295 3.1.5. Satellite altimetry

296 Water level fluctuations provided by altimetry missions can be used to monitor surface water  
297 reservoirs (e.g., river and lakes) height variations at global and regional scales (see, e.g., Awange  
298 et al., 2013; Tarpanelli et al., 2013; Paiva et al., 2013). Available products from Topex/Poseidon,  
299 Jason 1 and 2, and Envisat satellites are obtained from: <http://www.legos.obs-mip.fr/>. In  
300 this study, monthly lake variations are used to estimate surface water storage changes for Lakes  
301 Balbina, Tucuruí, and other main 6 lakes (reservoirs) in Brazil.

Table 4: Summary of the data sets used in this study.

Data	Period	Temporal resolution	Spatial resolution	References
GRACE	2002-2015	Monthly	$1^\circ \times 1^\circ$	Tapley et al. (2004)
TRMM	2002-2015	Monthly	$0.25^\circ \times 0.25^\circ$	Kummerow et al. (1998)
GLDAS	2002-2015	Monthly	$0.25^\circ \times 0.25^\circ$	Rodell et al. (2004)
WGHM	2002-2015	Monthly	$0.5^\circ \times 0.5^\circ$	Döll et al. (2014)
Altimetry	2002-2015	10-days		Cretaux et al. (2011)

## 302 3.2. Methodology

### 303 3.2.1. Groundwater changes derived from GRACE

304 Groundwater changes can be computed as:

$$\Delta GW = \Delta TWS - \Delta SM - \Delta CW - \Delta SW, \quad (1)$$

305 where  $\Delta GW$  are the groundwater changes,  $\Delta TWS$  the total water storage changes,  $\Delta SM$  the  
306 soil moisture changes,  $\Delta CW$  the canopy water changes and  $\Delta SW$  the surface water changes.  
307  $\Delta TWS$  are obtained from GRACE, while  $\Delta SM$  and  $\Delta CW$  are derived from GLDAS (see e.g.,  
308 Haohan et al., 2013; Nanteza et al., 2016). As for  $\Delta SW$ , many previous studies that computed  
309 GRACE-derived groundwater changes (e.g., Awange et al., 2014; Haohan et al., 2013) do not

310 consider surface water, given that they were often too small in their respective study areas.  
311 For Brazil, however, due to a large number of rivers and lakes located within the different  
312 regions of study,  $\Delta SW$  might be a significant part of  $\Delta TWS$  and could cause bias when we  
313 make conclusion without removing it. Therefore, it is necessary to calculate surface water  
314 contribution (rivers and lakes need to be estimated separately) for each region, and test how  
315 much influence it will bring to  $\Delta GW$ . In fact, the lake water storage changes and river water  
316 storage changes in most regions of the Brazil can be ignored, only the Amazon basin (region  
317 2) with large river water storage needs to be removed. The computations and results can be  
318 found in the Supporting Material (Section A). Here we only present the results of groundwater  
319 storage change time series for the Amazon basin, before and after removing the river water  
320 storage changes.

321 Figure 3a shows a river water storage distribution map over Brazil estimated using WGHM,  
322 while Figure 3b is a filtered version of Figure 3a after removing all the pixels consisting of water  
323 storage values smaller than the 300 mm. The 300 mm value was tested along side 100 mm and  
324 200 mm, and was finally selected as a threshold to distinguish the differences between large  
325 rivers and small streams. It is easily seen that the Amazon river is the main contributor of  
326 surface water storage in region 2 (see Figure 1a). River water storage in the rest of the study  
327 regions were ignored since they are relatively small (i.e., contributions to time series of less than  
328 0.5 cm). Figure 4 presents a comparison of the GRACE-derived groundwater storage changes  
329 ( $\Delta GW$ ) before and after removing the river water storage changes, and WGHM-derived  $\Delta GW$   
330 in region 2. The results show that the amplitude of the GRACE decreased by about 5 to 10 cm  
331 after removing the river water storage. However, there is still a significant difference between  
332 GRACE and WGHM-derived  $\Delta GW$  values in region 2. With such a difference in groundwater  
333 changes in region 2 derived by the two different products (GRACE and WGHM), it raises the  
334 issue of the accuracy of the used data sets. In the Supporting Material (Section B), a detailed  
335 evaluation of the two data sets is carried out.

336

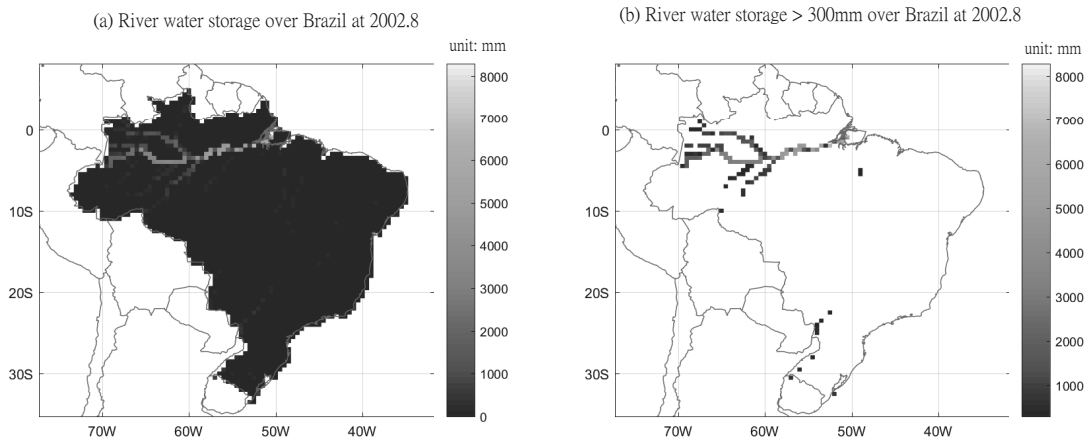


Figure 3: (a) River water storage map estimated by WGHM. (b) River water storage map filtered by removing areas less than 300mm. This is undertaken to filter out insignificant contributions from small rivers.

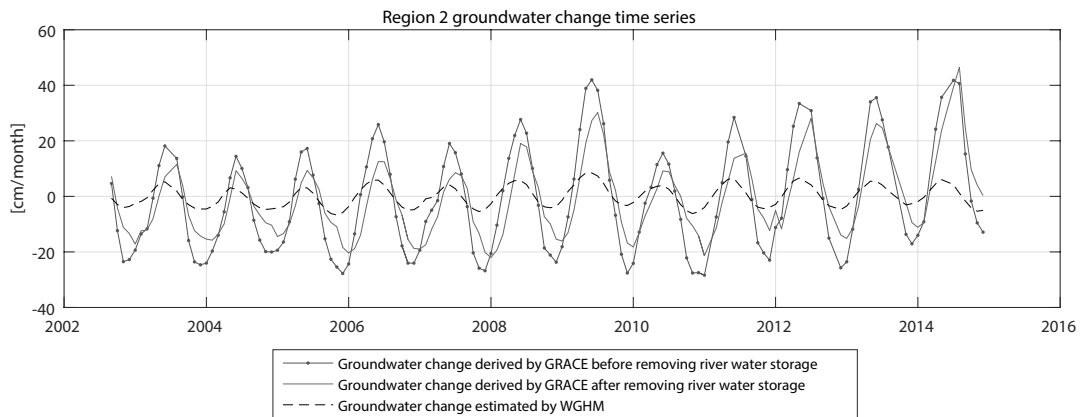


Figure 4: Region 2's groundwater changes derived from GRACE and WGHM products. After removing the surface water, the groundwater derived by GRACE decreased by 5 to 10 cm (i.e., the red line).

337 *3.2.2. Principle component analysis (PCA)*

338 Principal component analysis (PCA; Preisendorfer (1988)), widely applied in meteorology, is  
 339 a method employed to a group of time series data to reduce the dimension of multivariate data  
 340 in order to extract the most dominant variations in the original data set through the creation  
 341 of new variables with linear functions. Assuming a data matrix  $x_{i,k}$  contains rows representing

342 the time  $i$  (in months or days) and  $k$ , given  $k$  variables at a given time period  $i$ , the linear  
 343 combination for  $k$  principal components (PCs) is given by (Preisendorfer, 1988):

$$PCs = \begin{pmatrix} y_{i,1} = p_{11}x_{i,1} + p_{12}x_{i,2} + p_{13}x_{i,3} + \dots + p_{1k}x_{i,k} \\ y_{i,2} = p_{21}x_{i,1} + p_{22}x_{i,2} + p_{23}x_{i,3} + \dots + p_{2k}x_{i,k} \\ \dots \\ y_{i,k} = p_{k1}x_{i,1} + p_{k2}x_{i,2} + p_{k3}x_{i,3} + \dots + p_{kk}x_{i,k} \end{pmatrix}, i = 1, 2, \dots, n, \quad (2)$$

344 where  $y$  values are orthogonal  $PCs$  that explain variability from high ( $y_{i,1}$ ) to low ( $y_{i,k}$ ). The  
 345 eigenvalues ( $\lambda_1, \lambda_2, \dots$ ) corresponds to each eigenvector ( $p_{1,1}, p_{1,2}, \dots$ ), which explains the  
 346 fraction of the total variance explained by the loadings ( $p$ ). Further details can be found, e.g.,  
 347 in Preisendorfer (1988). In this study, the empirical orthogonal functions (EOFs) derived from  
 348 matrix  $x_{i,k}$  give EOF/PC pairs, are called PCA modes. The output of a PCA decomposition  
 349 give the trends and dominant spatio-temporal patterns of TWS, rainfall, and groundwater to  
 350 help evaluate the impact of rainfall on groundwater changes.

### 351 3.2.3. Box plot analysis

352 A box plot can be a convenient way of graphically depicting numerical data variability  
 353 (Rousseeuw et al., 1999), and indicates values of the maximum, minimum, medium and 1<sup>st</sup>  
 354 (i.e., 25%), 3<sup>rd</sup> (i.e., 75%) quartile. The interquartile range can be calculated as (Rousseeuw et  
 355 al., 1999):

$$\Delta Q = Q3 - Q1, \quad (3)$$

356 where the lowest and highest data are in the range of  $Q1 - 1.5\Delta Q$  to  $Q3 + 1.5\Delta Q$  (Tukey,  
 357 1977). Any data beyond this range are regarded as outliers. In this study, box plots are used  
 358 to analysis the relationship between rainfall and groundwater storage.

### 359 3.2.4. Cross-correlation analysis

360 Cross correlation is a standard method of evaluating the similarity to which two series are  
 361 linearly correlated. Assuming there are two series  $x_i$  and  $y_i$ , where  $i = 0, 1, 2, \dots$ , the correlation  
 362  $r$  at delay  $d$  is defined as (Bourke, 1996):

$$r = \frac{\sum_i (x_i - \bar{x})(y_i - \bar{y})}{\sqrt{\sum_i (x_i - \bar{x})^2} \sqrt{\sum_i (y_i - \bar{y})^2}} \quad (4)$$

363 where the  $\bar{x}$  and  $\bar{y}$  are the mean of correlated series.

364 To study the lag time and correlation of groundwater storage changes with rainfall, a corre-  
 365 lation analysis is carried out between GRACE-derived  $\Delta GW$  and precipitation. Also, a corre-  
 366 lation analysis between GRACE and WGHM-derived  $\Delta GW$  for validation purpose is presented  
 367 in Supporting Material (Section A).

### 368 3.2.5. Comparison between aquifer recharge and discharge speeds

369 The groundwater table level will raise and fall in wet and dry seasons, respectively, consid-  
 370 ering rainfall as a major source. However, different rock formations will have different recharge  
 371 and discharge speeds due to the rock properties, layer structures and elevation impacts. The  
 372 ‘dam’ reservoir pattern (see section 2.4 and Table 3) is such a special phenomenon, which indi-  
 373 cates large potential of groundwater volume given that it has a strong ability to hold water with  
 374 a rapid response of recharge, but slow rate of discharge. It is necessary, therefore, to compare  
 375 the groundwater recharge rates in wet seasons to discharge in dry seasons in order to test the  
 376 ability of holding groundwater in different regions. In this case, all the 138 months of ground-  
 377 water changes employed are distributed and divided into increasing and decreasing parts. The  
 378 values are then sorted from low to high for the increasing parts, and from high to low for the  
 379 decreasing parts and plotted separately. The slopes of the increasing and decreasing parts are  
 380 then compared to give recharge and discharge speeds. A single value of slope is calculated as  
 381 (modified to the case of groundwater change from Sawicz et al., 2011):

$$S = \frac{\Delta GW(2/3_{rd}) - \Delta GW(1/3_{rd})}{N(2/3_{rd}) - N(1/3_{rd})}, \text{ wet season,} \quad (5)$$

$$S = \frac{\Delta GW(1/3_{rd}) - \Delta GW(2/3_{rd})}{N(2/3_{rd}) - N(1/3_{rd})}, \text{ dry season,} \quad (6)$$

382 where  $S$ , is the slope which reflects the speed of recharge (Eq. 5) and discharge (Eq. 6),  $\Delta GW$   
 383  $1/3_{rd}$  is the one third value of increasing or decreasing parts,  $N$  is the data number count  
 384 of increasing and decreasing part, respectively. The higher values of groundwater change in

385 slope plot may be attributed to extreme rainfall and the lower values may be subject of severe  
386 drought throughout the period of analysis. For this reason, the slope is calculated in a range  
387 where variation is not greatly subjected to both extremes such as between the  $1/3_{rd}$  and  $2/3_{rd}$   
388 groundwater value in order to avoid bias.

## 389 4. Results and discussion

### 390 4.1. Spatial temporal variability of groundwater over Brazil

391 Seasonal and annual rainfall mainly control groundwater change trends (i.e., increase in  
392 wet season and decrease in dry season), given that it provides a large part of the incoming  
393 water. To evaluate its impact on groundwater changes over Brazil, principle component analysis  
394 (PCA) was carried out (Figure 5) to infer the effect of rainfall/rock property relationships on  
395 groundwater changes. Figure 5 presents the first three dominant components of rainfall, TWS  
396 changes ( $\Delta TWS$ ) and groundwater changes ( $\Delta GW$ ), which explain over 90% of the variability  
397 of each product.

398 In the first principle component (PC1), rainfall,  $\Delta TWS$  and  $\Delta GW$  capture the annual  
399 signals over Brazil, with rainfall (73.4% variability) showing extreme climate in the central  
400 parts of Brazil, which varies greatly (amplitude reach to 30 cm) between wet and dry seasons.  
401 Nevertheless, when it goes towards the coast, such as in regions 5 and 8 (south and northeast  
402 coastal areas, respectively), the amplitude becomes smaller (approximately 0 to 5 cm). For  
403  $\Delta TWS$  (74.9% variability), a strong variation (amplitude from 20 to 40 cm) in northern Brazil,  
404 which corresponds to regions 1, 2, 3 and partly 4 and 6 is seen. Variation in the coastal regions  
405 5, 8 and 9 are rather small (amplitude from 0 to 10 cm). The results of  $\Delta TWS$  basically matches  
406 those of  $\Delta GW$  (81.0% variability), which demonstrates the fact that groundwater comprises a  
407 major part of the total water storage, and its spatial variabilities are less affected by rainfall.

408 In PC2, rainfall shows a seasonal variations (have increasing and decreasing trends in each  
409 season of year) while the  $\Delta TWS$  and  $\Delta GW$  time series still show annual trends, which could  
410 mean that seasonal rainfall variations does not affect  $\Delta TWS$  and  $\Delta GW$  much. Also, from  
411 EOFs of rainfall (21.3% variability), opposite rainfall trends between the northern and southern  
412 Brazil is noticeable, with the Amazon river (approximately) acting as the boundary. A similar  
413 pattern emerges with  $\Delta TWS$  (19.8% variability). This proves that rainfall will influence spatial

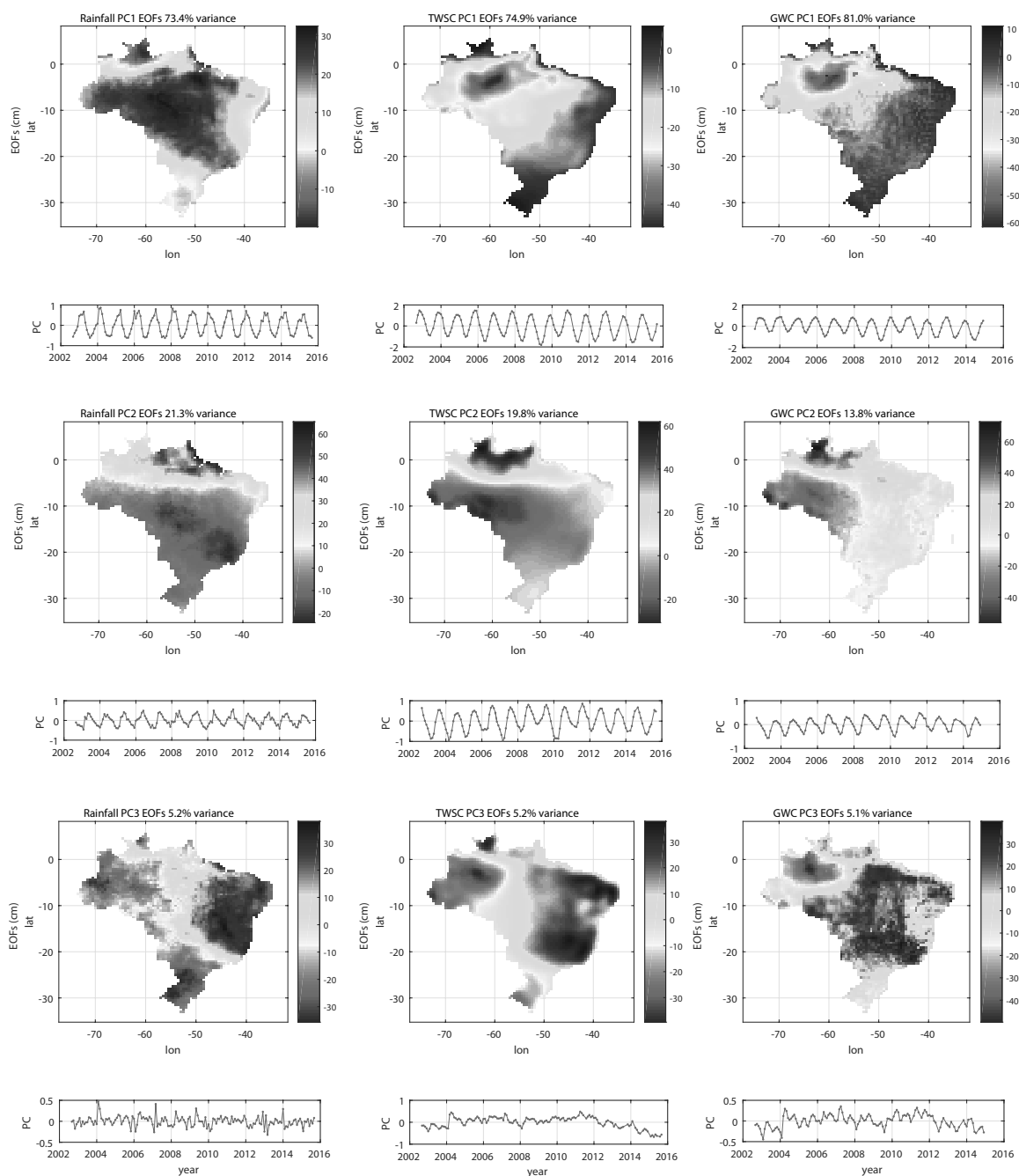


Figure 5: PCA analysis, comparison of (from left to right) rainfall, TWS, groundwater change patterns. PC1 indicates that rainfall is less affected on groundwater spatial distribution, PC2 depicts that surface water, soil moisture and canopy water are easier influenced by rainfall than groundwater, while PC3 shows the west of the west of region 2 in the Amazon basin kept losing water from 2002 to 2008.



414 distribution of surface water, soil moisture and canopy water in some extend, but has less  
415 influence on groundwater. This is due to the fact that EOFs of  $\Delta GW$  does not match with  
416 those of rainfall and  $\Delta TWS$  as seen from PC2s in Figure 5 (row 2). Besides,  $\Delta TWS$  reveals  
417 the droughts of 2003-2004, 2005 and 2010 that occurred in the north and northeast Brazil,  
418 confirming the findings of Frappart et al. (2011) and Marengo et al. (2016). Rainfall and  
419  $\Delta GW$ , however, do not show obvious signs of droughts over the same period of time. This  
420 could possibly imply that those droughts affected mainly the surface water and soil moisture  
421 captured by changes in TWS compared to groundwater. In addition, EOFs of  $\Delta GW$  also  
422 reveals that the whole region 1 (i.e., the region beyond northern side of the Amazon aquifer)  
423 keeps losing water from 2002 to 2008 considering the PCs are negative mostly in the same time  
424 period. This results matches well with groundwater accumulation analysis in Figure 5 in the  
425 Supporting Material (Section C).

426 In PC3, the EOFs of rainfall (5.2% variability) and  $\Delta TWS$  (5.2% variability) matches well,  
427 with both showing that the there are opposite trends between western and eastern Brazil. More  
428 importantly, in PC3, most values of the PCs in  $\Delta TWS$  and  $\Delta GW$  are positive from 2004 to  
429 2012, which shows that the west of region 2 in the Amazon basin kept losing water during this  
430 period (compare these results with those of Figure 5 in the Supporting Material, Section C).

#### 431 4.2. Groundwater variation in relation to flow direction

432 Figure 6 shows groundwater and rainfall time series from 2002 to 2015 over the 9 study  
433 regions of Brazil. As the main source of water for all regions, the rainfall changes in regions 1  
434 to 4 (the Amazon region) are almost of the same amplitude compared to those of groundwater  
435 changes. This is a surprising phenomenon since one would expect the amplitudes of groundwater  
436 variation to be smaller than those of rainfall due to the fact that rainfall is considered to be the  
437 main source of groundwater recharge. However, for regions 1 to 4, this is not the case, probably  
438 due to some other significant source of water (e.g., groundwater flowing from other regions).

439 In section 2.1 (Figure 1d), a general flow direction of groundwater and surface water in  
440 Brazil was presented. In region 1, there is extra groundwater coming from the north of the  
441 country, from areas such as Guyana, Suriname and French Guiana. Region 2 has the biggest  
442 river (the Amazon river) in Brazil, with the headstream that comes from west of Peru. Also,  
443 regions 1 and 3 provide groundwater and surface water to region 2, especially for the aquifer

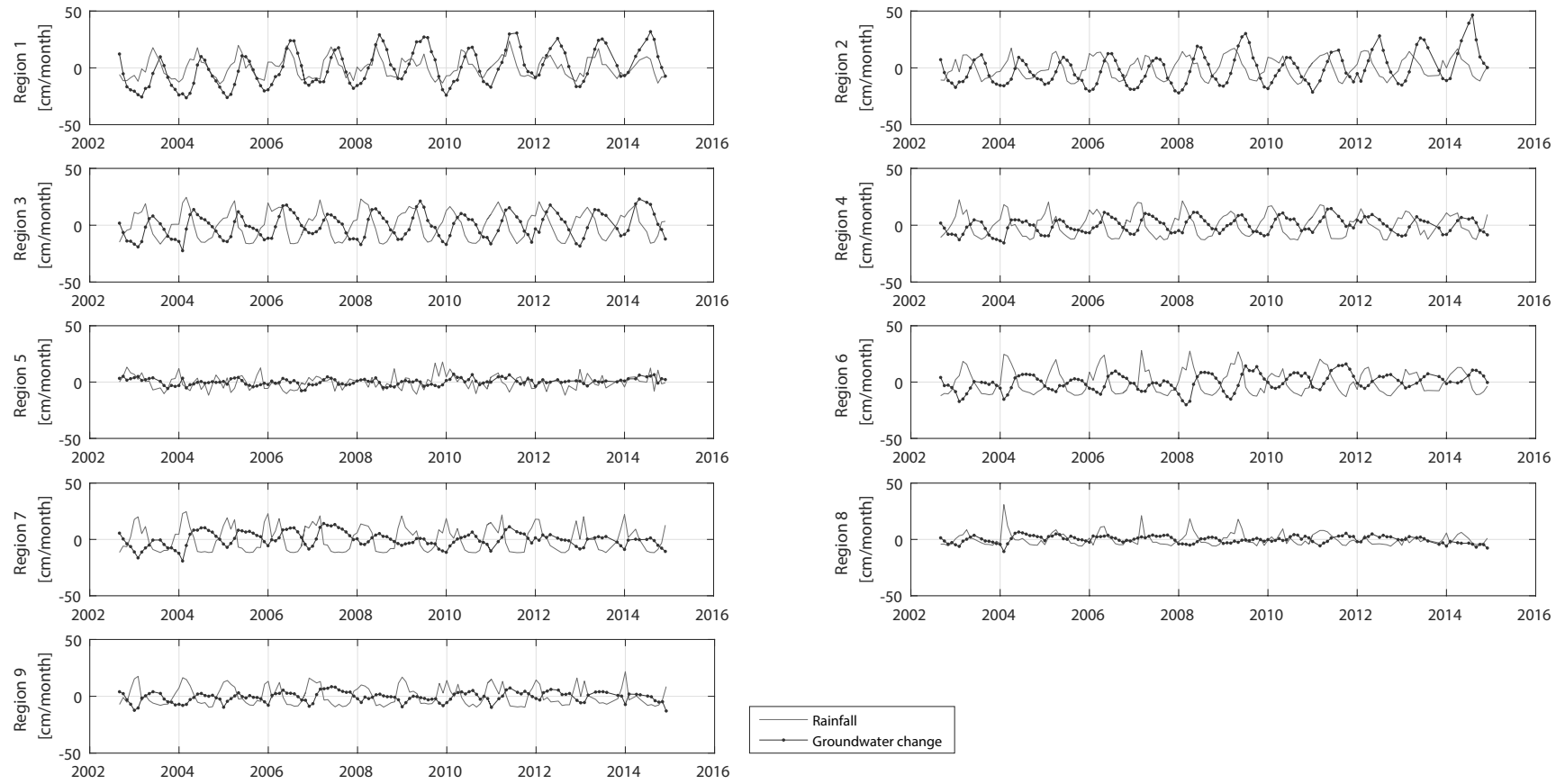


Figure 6: Time series of rainfall and groundwater changes over the study regions in Brazil. Regions 1 to 4 show that there are almost same amplitudes between rainfall and groundwater changes, which indicates these regions are receiving extra water from other regions.

444 Alter do Chão. The difference in amplitude between groundwater and rainfall in region 3 is  
445 smaller compared to regions 1 and 2, which still receives extra incoming water from regions  
446 4 and 7. In region 4, groundwater and rainfall variations are almost equal, with the water is  
447 coming from regions 5, 7 and 9, although the quantity is a bit of small.

448 Therefore, the Amazon basin is the largest potential groundwater reservoir from the per-  
449 spective of water flow in Brazil. On the other hand, rainfall and groundwater amplitudes in  
450 regions 4, 6, and 7 are relatively small compared to those of regions 1 to 3, while regions 5,  
451 8 and 9 have the smallest variations compared to the other regions. This is possibly due to  
452 insufficient rainfall as source of groundwater and the small groundwater storage capacity of  
453 those regions, which will be discussed in Section 4.3.

#### 454 *4.3. Groundwater storage capacity*

455 Rainfall, as main source of groundwater, determines groundwater storage to a large extend,  
456 unless the storage capacity of areas are very small due to the limitation of rock properties.  
457 To identify the groundwater storage capacity of each region, rainfall and groundwater changes  
458 are compared in Figure 7. Also, Table 5 combines the geological properties and groundwater  
459 changes for a convenient view to identify groundwater storage capacity (the ability to hold  
460 groundwater will be discussed in Section 4.4).

461 According to Figure 7, the medium values (red lines) and box range show that regions 1,  
462 2 and 3 (the Amazon region) have the highest rainfall values among all the regions about 10  
463 to 20 cm. The Amazon region, therefore, can be said to have the largest groundwater storage  
464 capacity over Brazil is already pointed out in Section 4.2. More specifically, regions 1 and 3 are  
465 comprised of fractured rock types in which the groundwater storage conditions and capacity  
466 are not expected to be stable, nor be as large as that of the granular rock formation in region 2  
467 (see Table 5). However, a similar variation pattern is seen in these three regions, possibly due  
468 to the fact that regions 1 and 3 display a ‘dam’ pattern, as discussed in Section 4.4. The range  
469 of medium rainfall values in regions 4, 5, 6 and 7 are from 10 to 15 cm. Regions 8 and 9 along  
470 the coastal areas have the smallest medium rainfall values (approx. 5 to 10 cm). One can see  
471 that although region 5 (part of the Guarani aquifer) has the smallest groundwater variation,  
472 its rainfall is higher than in regions 8 and 9 (lower groundwater change regions, see Figure  
473 6). By reviewing Section 2.3 and Figure 1b, it is not hard to see that the very limited direct

474 recharge area (Botucatu and Piramboia layers exposed on the surface) is the reason why the  
 475 groundwater water variation in region 5 is so small and stable. To more accurately evaluate  
 476 region 5's groundwater volume, in-situ data, such as water table height time series observed  
 477 from local wells, are needed. Meanwhile, regions 8 and 9 have low groundwater storage capacity  
 478 due the fact that they have low rainfall recharge (see Figure 7).

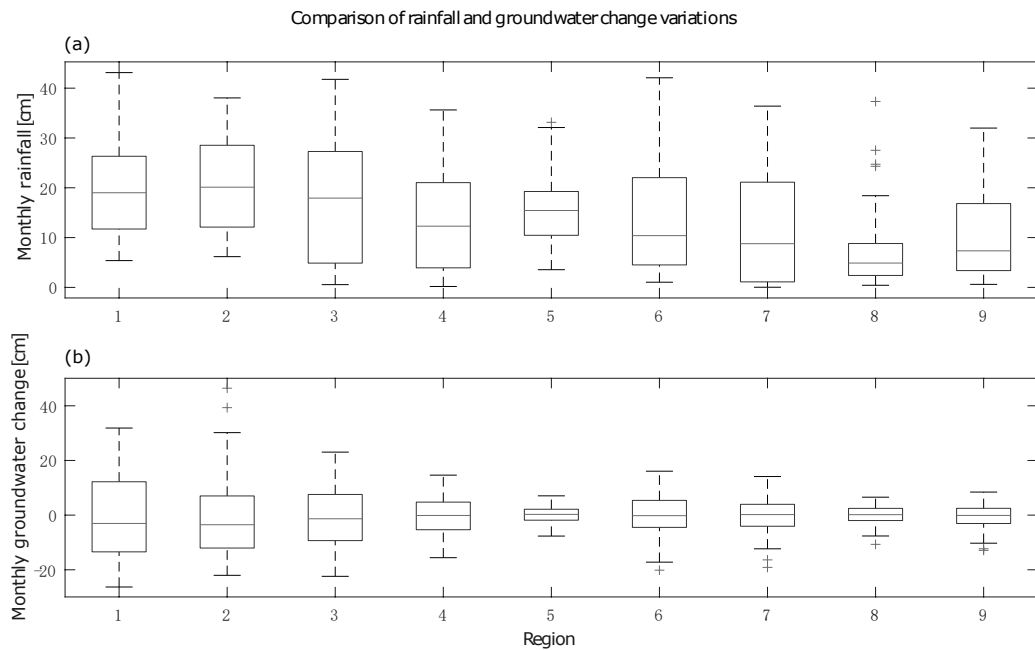


Figure 7: Comparison of monthly rainfall and groundwater changes over the study region. The red crosses indicates outliers. The lower tail of the box plots indicate the smallest observation (sample minimum), the lower end of the box shows the lower quartile (25%), the line across the box indicates the median, the upper end of the box specify the upper quartile (75%), and the upper tail of the plots illustrate the largest observations (sample maximum).

479 Comparing Tables 1 and 3, almost all the main aquifer layers in each region, except region  
 480 7, belong to the granular rock types. According to Ricardo and Bruno (2011), the Urucuia  
 481 aquifer in region 7 is made up of granular rocks with a permeability greater than  $10^{-4}$ . On the  
 482 one hand, although the Bambui aquifer is located in an area with vast karst terrain, consisting  
 483 of limestones with extremely well developed fractures, it still provides good conditions for  
 484 groundwater movement and storage capability. On the other hand, for the biggest two aquifer  
 485 systems in Brazil (Amazon and Guarani aquifers), the main aquifer layers, Alter do Chão and

Table 5: Geological properties linked to groundwater changes over Brazil.

Regions	Aquifer	Rock type*	Rainfall medium (cm)	Permeability# average(m/s)	GW Variation amplitude (cm)	Ability of holding GW RS-DS <sup>+</sup>
1	N/A	Fractured	20	$10^{-8}$ to $10^{-7}$	30	0.29
2	Amazon aquifer	Granular	20	$\geq 10^{-4}$	30	0.14
3	N/A	Fractured	20	$10^{-8}$ to $10^{-7}$	25	0.44
4	Guarani and Pantanal	Granular	10 to 15	$\geq 10^{-4}$	10 to 15	0.14
5	Guarani aquifer	Granular	10 to 15	$10^{-6}$ to $10^{-4}$	below 5	N/A
6	Itapecuru, Piaui	Granular	10 to 15	$10^{-6}$ to $10^{-4}$	10 to 15	0.08
7	Urucuia and Bambui	Fractured/Granular	10 to 15	$\geq 10^{-4}$	10 to 15	-0.01
8	N/A	Fractured	below 10	$10^{-8}$ to $10^{-7}$	below 5	N/A
9	N/A	Fractured	below 10	$10^{-8}$ to $10^{-7}$	below 8	N/A

Note:

1)\* Regions 4 and 5 rock layers consist of both granular and fractured rocks. However, the main aquifer layers are granular rocks, so we define these aquifers as granular. Furthermore, region 7 has both granular and fractured rocks as the main aquifer formations;

2)# Permeability given in this table is only for the main rock layer that contains groundwater and the results should be interpreted with caution;

3)<sup>+</sup> RS-DS is the difference between Recharge Slope (SR) and Discharge Slope (DS).

486 Botucatu & Piramboia, also have a permeability equal to or over  $10^{-4}$ , which indicate large  
487 groundwater storage potential (see Table 3).

#### 488 *4.4. Aquifer recharge/discharge mechanism*

489 The observed lags between groundwater changes and rainfall represent the time that rainfall  
490 takes to filtrate into the ground. Table 6 summarise the lags and correlations between ground-  
491 water and rainfall changes over the study region (at a 95% confidence level). Higher lag periods  
492 are indicative of indirect recharge mechanisms, which refers to the strong ability of holding  
493 groundwater, and small storage capacity, while smaller values are more likely to be attributed  
494 to direct recharge mechanisms (rapid response to rainfall and large storage capacity potential).  
495 The results show that the Amazon regions 1 to 3 and region 4 have the highest correlations,  
496 above 0.70, which can be attributed to the direct recharge mechanism (region 2 receives a large  
497 amount of groundwater from other areas, so it should be regarded as being recharged by both  
498 direct and indirect mechanisms). Regions 6, 7 and 9 have values lower than 0.70, and can be  
499 regarded as being indirectly recharged. The correlations in regions 5 and 8 are the smallest,  
500 with only around 0.38 and 0.29 (not significant), respectively. It seems that rainfall does not  
501 influence groundwater changes in these two regions. As for the lags, region 1 has the fastest  
502 groundwater response speed, which only takes one month to detect when the incoming rainfall  
503 becomes groundwater. For regions 2 to 5, this is slightly longer, with lags of 3 months. The  
504 coastline regions 8 and 9 have 4 months lag, while regions 6 and 7 have the longest observed  
505 lags between rainfall and groundwater, i.e., 5 months. In addition, except regions 5 and 8, all  
506 the correlations between rainfall and groundwater changes are above 0.5. This indicates that  
507 rainfall, as main source of groundwater, controls groundwater trends to a large extend (i.e.,  
508 increase in wet season and decrease in dry season).

509 In Section 2.4, the ‘dam’ reservoir pattern was defined as an area with rapid groundwater  
510 increasing rates, but slow outflow. To compare the recharge and discharge speeds of ground-  
511 water, Figure 8 organised all the 138 months of groundwater values by separating increasing  
512 (wet seasons) and decreasing (dry seasons) parts. The slopes are then computed using Eqs.  
513 5 and 6 and are presented in Table 7. The recharge/discharge slopes reflect the flow rate in  
514 wet/dry seasons (increasing/decreasing parts in Figure 8). Due to the fact that regions 8 and 9  
515 are located along the coastline, and their groundwater changes and the incoming rainfall very  
516 small, there exists no possibility of large groundwater storage potential in these two areas. The

Table 6: Cross-correlation summary for all regions. The correlations are with respect to the lags at 95% confidence level. The none-significant correlations are marked by an asterisk\*.

Regions	Rainfall vs GWC (lags/months)	Correlation	Recharge Mechanism
1	1	0.752	direct dominant
2	3	0.793	both direct and indirect dominant
3	3	0.762	direct dominant
4	3	0.732	direct dominant
5	3	0.379*	indirect dominant
6	5	0.683	indirect dominant
7	5	0.562	indirect dominant
8	4	0.286*	indirect dominant
9	4	0.567	indirect dominant

517 recharge and discharge speeds in these two regions are therefore not examined further. As for  
518 region 5 (part of the Guarani aquifer), according to the PCA results presented in Figure 5 and  
519 the annual variation shown in Figure 6, it is very hard to track its groundwater increasing and  
520 decreasing trends due to the fact that there is obviously no annual rainfall and groundwater  
521 variation trends.

522 From Figure 8 and Table 7, regions 1 and 3 performed exactly as expected (e.g., Table 3),  
523 with ‘dam’ reservoir patterns of groundwater recharge slopes of 0.85 and 0.75, but 0.56 and  
524 0.31 for discharge slopes, respectively. Regions 2, 4, and 6 also show good ability for holding  
525 water with the difference ranging from 0.10 to 0.15 between recharge and discharge speeds.  
526 This is because regions 2 and 6 are linked to the Atlantic Ocean, which plays the role of a ‘wall’  
527 due to the fact that the water tables in these regions will always keep the same level with sea  
528 surface level at the edges of the coastline. As for region 4, its western domain is the plateau of  
529 Altiplano, with an elevation of about 2000 m. The only opening to which groundwater can flow  
530 out is through the southwestern part of the region, hence its ‘dam’ reservoir pattern appearance.

531 In addition, it is important to note that for all the regions, the number of months taken for  
532 the groundwater to increase part was much less than that of the number of months taken for

533 the groundwater to decrease (Figure 8). For example, regions 1, 2, 6 and 7 take about 60 to  
534 65 months (about 46%) for groundwater to increase, and 73 to 78 months (about 54%) for it  
535 to decrease. Greater differences appear in regions 3 and 4, which have only about 50 months  
536 (about 36%) of the increasing trends from the 138 months of data sets. Therefore, even though  
537 the 'dam' reservoir pattern has a strong ability to hold water, it might still keep losing water  
538 every year in those regions due to lack of rainfall. Also human consumption might be another  
539 important factor to lead lose of groundwater. Those hypotheses are discussed and identified  
540 in the Supporting Material (see, Section C). The results show that for the Amazon regions 1  
541 and 2, it kept losing groundwater from 2002 to 2008 due to lack of rainfall, while the impact of  
542 human water consumption is not significant over Brazil.



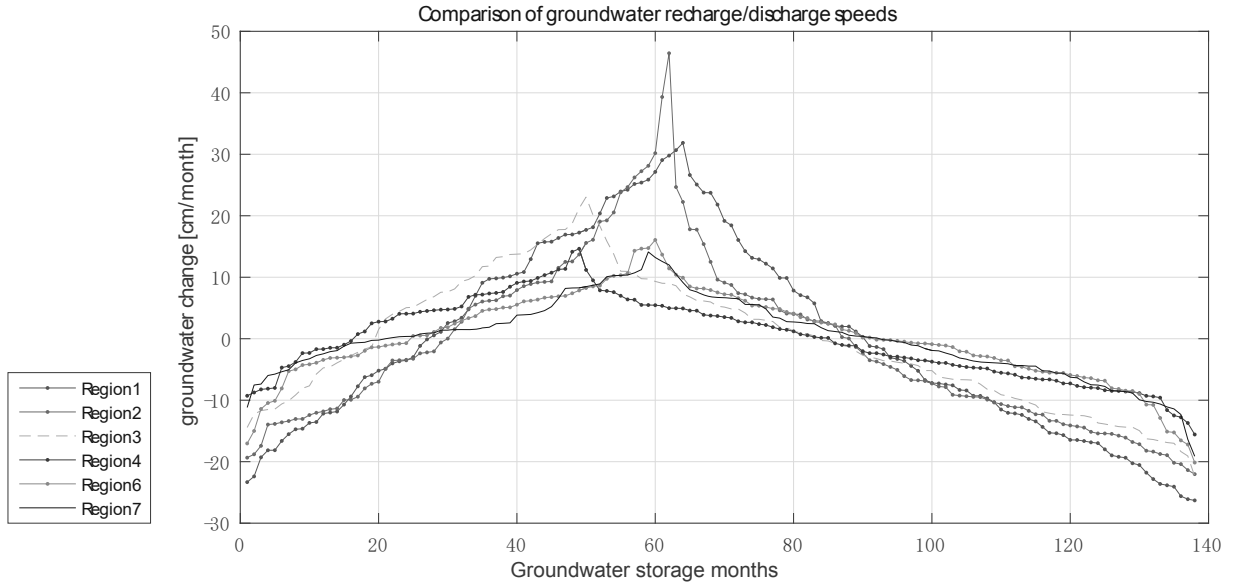


Figure 8: Comparison of recharge and discharge speeds of groundwater. Up to the 60th storage month, groundwater experiences trend of increase. Thereafter, up to the 138th month, there is a decrease (i.e., discharge).

Table 7: Recharge and discharge speed slope results based on Figure 8.

Regions	1	2	3	4	6	7
Recharge slope	0.85	0.58	0.75	0.35	0.34	0.20
Discharge slope	0.56	0.45	0.31	0.21	0.26	0.21

## 543 5. Conclusion

544 This study investigated the relationship between GRACE-derived groundwater changes and  
 545 geological conditions such as rock properties and aquifer types across Brazil in order to study  
 546 the groundwater potentials. By dividing the study area into 9 regions based on granular and  
 547 fractured rock types, the results indicated that:

- 548 (i) From the analysis of groundwater variations and rainfall, the Amazon aquifer was found to  
 549 have the largest groundwater storage capacity with the rock layers of highest permeability.

550 Guarani aquifer and east coastline inland domains follow, while coastal regions have the  
551 smallest groundwater storage capacity.

552 (ii) Groundwater changes suffer less from seasonal and annual rainfall variations than total  
553 water storage (TWS) over Brazil. This was evident from the Principal Component Anal-  
554 ysis (PCA) results, and therefore, geological characteristics could be the main factor that  
555 controls groundwater changes rates and storage capacity, rainfall, as source of groundwa-  
556 ter, only controls the increasing/decreasing trends.

557 (iii) The two main aquifer formations (Alter do Chão in the Amazon aquifer, Botucatu and  
558 Piramboia in the Guarani aquifer) that contribute to groundwater changes belong to the  
559 granular rock type, in contrast to fractured rocks which provide more stable conditions  
560 and larger space to support groundwater flow. Only the Bambui aquifer (region 7) is made  
561 of fractured rocks that have large potential capacity to store groundwater.

562 (iv) Groundwater over the Amazon region was found to be not only recharged by rainfall, but  
563 also inflow of groundwater from other regions.

564 (v) Although regions adjacent to the northern and southern Amazon basin do not contain  
565 any aquifer system, the groundwater recharge rates in these two regions are much faster  
566 than the discharge speed (defined as the ‘dam’ pattern). A large amount of groundwater  
567 can not go through both northern and southern edges of Alter do Chão due to the fact  
568 that there are two impermeable rock layers acting like ‘walls’, preventing water flowing  
569 through them.

570 (vi) Although rainfall in Guarani aquifer is substantial, the very limited direct recharge areas  
571 (Botucatu and Piramboia aquifer layers exposed at the surface) of the ‘basin’ pattern is  
572 the reason that contributes to small changes in groundwater.

573 (vii) For the Amazon regions, the study found that the lose of water experienced from 2002  
574 to 2008 was due to climatic variability, e.g., lack of rainfall. Geological characteristics  
575 were found not to have a significant contribution in this loss. The human consumption  
576 could not have significant contribution to the loss either, which had been proved by our  
577 WGHM results that corroborated those of Feick et al. (2005) (see details in the Supporting  
578 Material).

579 **Acknowledgements**

580 The authors are grateful to the following organizations for providing the data used in this  
581 study CSR, NASA, USGS, GES-DISC, Hydro-web and CPRM Brazilian government. Many  
582 thanks to Nathan, Chris and Mehdi of Curtin Universtiy for providing valuable comments  
583 during data processing. Joseph and Rodrigo are grateful for the Brazilian Science Without  
584 Borders Program/CAPES Grant No. 88881.068057/2014-01, which supported this study and  
585 the stay of the Joseph at UFPE Federal University of Pernambuco, Brazil. Rodrigo also would  
586 like to thank the support of CNPq Grant No. 310412/2015-3/PQ level 2.

587 **References**

- 588 Abelen, S., Seitz, F., Abarca-del-Rio, R., and Güntner, A. (2015). Droughts and floods in  
589 the la plata basin in soil moisture data and GRACE. *Remote Sensing*, 7(6), 7324–7349,  
590 doi:10.3390/rs70607324.
- 591 Alisson, E. (2014). Amazonia has an "underground ocean". Access from [http://agencia.fapesp.br/amazonia\\_has\\_an\\_underground\\_ocean/19679/](http://agencia.fapesp.br/amazonia_has_an_underground_ocean/19679/) on July 29, 2016.
- 593 Andersen, O. B., Seneviratne, I., Hinderer, J. and Viterbo, P. (2005). GRACE-derived terrestrial  
594 water storage depletion associated with 2003 European heat wave. *Geophysical Research*  
595 *Letters*, 32(18), L18405, doi:10.1029/2005GL023574.
- 596 Awange, J. L., Forootan, E., Kusche, J., Kiema, J. B. K., Omondi, P. A., Heck, B., Fleming, K.,  
597 Ohanya, S. O. and Gonçalves, R. M. (2013). Understanding the decline of water storage across  
598 the Ramser-Lake Naivasha using satellite-based methods. *Advances in Water Resources*, 60,  
599 7–23, doi:10.1016/j.advwatres.2013.07.002.
- 600 Awange, J. L., Gebremichael, M., Forootan, E., Wakbulcho, G., Anyah, R., Ferreira, V. G.  
601 and Alemayehu, T. (2014). Characterization of Ethiopian mega hydrogeological regimes  
602 using GRACE, TRMM and GLDAS datasets. *Advances in Water Resources*, 74, 64–78,  
603 doi:10.1016/j.advwatres.2014.07.012.
- 604 Awange, J. L., Mpelasoka, F., Goncalves, R. M. (2016). When every drop counts: Analysis of  
605 Droughts in Brazil for the 1901-2013 period. *Science of the Total Environment*, 1472(88),  
606 566–567, doi:10.1016/j.scitotenv.2016.06.031.
- 607 Bahniuk, A. M., Matsuda, N. S., Neto, J. M. R., Franca, A B, Jahnert R J, Juschaks, L. (2008).  
608 Geological and geomorphological elements in the karst systems; Precambrian acungui group,  
609 Southern Brazil. *33<sup>rd</sup> International Geological Congress*, 33. Access from <http://search.proquest.com.dbgw.lis.curtin.edu.au/> on July 21, 2016.
- 611 Birkinshaw, S. and Moore, P. (2014). CRYosat-2 sUCcess over Inland water And Land. *New-*  
612 *castle University*, 1, 1–45.
- 613 Bourke, P. (1996). Cross Correlation. Access from <http://paulbourke.net/miscellaneous/correlate/> on November 13, 2016.

- 615 Broad, K., Pfaff, A., Taddei, R., Sankarasubramanian, A., Lall, U., Assis, S. F. (2007). Cli-  
616 mate, stream flow prediction and water management in northeast Brazil: Societal trends and  
617 forecast value. *Climatic Change*, 84(2), 217–239, doi:10.1007/s10584-007-9257-0.
- 618 Cameron, J. (2012). Groundwater Essentials. *National Water Commission*, pp. 1–48. Access  
619 from [http://www.groundwater.com.au/.../Groundwater\\_essentials.pdf](http://www.groundwater.com.au/.../Groundwater_essentials.pdf) on September  
620 14, 2016.
- 621 Cao, Y., Nan, Z., & Cheng, G. (2015). GRACE gravity satellite observations of terrestrial water  
622 storage changes for drought characterisation in the arid land of Northwest China. *Remote*  
623 *Sensing*, 7(1), 1021–1047, doi:10.3390/rs70101021.
- 624 Castellazzi, P., Martel, R., Galloway, D. L., Longuevergne, L. and Rivera, A. (2016) Assessing  
625 Groundwater Depletion and Dynamics Using GRACE and InSAR: Potential and Limitations.  
626 *Groundwater*, pp. 1–13, doi:10.1111/gwat.12453.
- 627 Charles, J. T., William, M. A. (2001). Ground-Water-Level Monitoring and the Importance of  
628 Long-Term Water-Level Data. *U.S. Geological Survey*. Access from [http://pubs.usgs.gov/  
629 circ/circ1217/pdf/circ1217\\_final.pdf](http://pubs.usgs.gov/circ/circ1217/pdf/circ1217_final.pdf) on September 11, 2016.
- 630 CPRM. (2014). Map of Hydrogeology of Brazil. *Brazil geology service*. Accessed from [http:  
631 //geobank.cprm.gov.br/](http://geobank.cprm.gov.br/) on August 17, 2016.
- 632 Cretaux, J. F., Jelinski, W., Calmant, S., et al. (2011). A lake database to monitor in the Near  
633 Real Time water level and storage variations from remote sensing data. *Advances in space*  
634 *Research*, 47, 1497–1507, doi:10.1016/j.asr.2011.01.004.
- 635 Döll, P., Schmied, M. C., Schuh, C., Portmann, F. T. and Eicker, A. (2014). Global-scale assess-  
636 ment of groundwater depletion and related groundwater abstractions: Combining hydrologi-  
637 cal modeling with information from well observations and grace satellites. *Water Resources*  
638 *Research*, 50(7), 5698–5720, doi:10.1002/2014WR015595.
- 639 Döll, P., Douville, H., Güntner, A., Schmied, H. M. and Wada, Y. (2015). Modelling Freshwater  
640 Resources at the Global Scale: Challenges and Prospects. *Surveys in Geophysics*, 37, 1–27,  
641 doi:10.1007/s10712-015-9343-1.
- 642 Eliene, L.S., Paulo, H. F. G., Cleane, S. S. P., Marcus, P. M. B., José, G. A. D. and  
643 Wilker R. R. B. (2013). Sintese da hidrogeologia nas bacias sedimentares do Amazonas e

- 644 do Solimões: Sistemas Aquíferos Icó-Solimões e Alter do Chão. *Geosciences USP*, 13(1),  
645 107–117, doi:10.5327/Z1519-874X2013000100007.
- 646 Farlin, J., Drouet, L., Galle, T., ...Kies, A. (2013). Delineating spring recharge areas in a  
647 fractured sandstone aquifer (Luxembourg) based on pesticide mass balance. *Hydrogeology*  
648 *Journal*, 21(4), 799–812.
- 649 Feick, S., Siebert, S., and Döll, P. (2005). Global map of artificially drained agricultural areas,  
650 *University of Frankfurt (Main), Germany*, Accessed from [http://www.uni-frankfurt.de/](http://www.uni-frankfurt.de/45217895/2_agricultural_drainage_map)  
651 [45217895/2\\_agricultural\\_drainage\\_map](http://www.uni-frankfurt.de/45217895/2_agricultural_drainage_map) on October 29, 2016.
- 652 Ferreira, V. G., Gong, Z. and Andam-Akorful, S. A. (2012). Monitoring mass changes in the  
653 Volta River basin using GRACE satellite gravity and TRMM precipitation, *Bol. Ciênc. Geod.*,  
654 18(4), 549–563, doi:<http://dx.doi.org/10.1590/S1982-21702012000400003>.
- 655 Filho, O. A. S., Silva, A. M., Remacre, A. Z., Sancevero, S. S., McCafferty, A. E. and Per-  
656 rotta, M. M. (2010). Using helicopter electromagnetic data to predict groundwater quality in  
657 fractured crystalline bedrock in a semi-arid region, northeast Brazil. *Hydrogeology Journal*,  
658 18(4), 905–916, doi:10.1007/s10040-010-0582-4.
- 659 Forootan, E., Rietbrok, R., Kusche, J., Sharifi, M. A., Awange, J. L., Schmidt, M., Omondi,  
660 P and Famiglietti, J. (2014). Separation of large scale water storage patterns over Iran using  
661 GRACE, altimetry and hydrological data. *Remote Sensing of Environment*, 140, 580–595,  
662 doi:10.1016/j.rse.2013.09.025.
- 663 Frappart, F., Papa, F., Guntner, A., Werth, S., da Silva, J. S, Tomasella, J., Seyler, F.,  
664 Prigent, C., Rossow., W. B., Calmant, S., Bonnet, M. P. (2011). Satellite-based estimates of  
665 groundwater storage variations in large drainage basins with extensive floodplains. *Remote*  
666 *Sensing of Environment*, 115, 1588–1594, doi:10.1016/j.rse.2011.02.003.
- 667 Freeze, R. A., Witherspoon, P. A. (1967). Theoretical analysis of regional groundwater flow:  
668 2. Effect of water-table configuration and subsurface permeability variation. *Water resource*  
669 *research*, 3(2), 623–624, doi:10.1029/WR003i002p00623.
- 670 Friedel, M. J., de, S. F., Iwashita, F., Silva, A. M., and Yoshinaga, S. (2012). Data-driven  
671 modeling for groundwater exploration in fractured crystalline terrain, northeast Brazil. *Hy-*  
672 *drogeology Journal*, 20(6), 1061–1080, doi:10.1007/s10040-012-0855-1.

- 673 Gastmans, D., Hutcheon, L., Menegàrio, A. A. and Chang, H. K. (2016). Geochemical evolution  
674 of groundwater in a basaltic aquifer based on chemical and stable isotopic data: Case study  
675 from the Northeastern portion of Serra Geral Aquifer, São Paulo state (Brazil). *Journal of*  
676 *Hydrogeology*, 535, 598–611, doi:http://dx.doi.org/10.1016/j.jhydrol.2016.02.016.
- 677 Getirana, A. (2015). Extreme Water Deficit in Brazil Dected from Space. *Journal of Hydrom-*  
678 *eteorology*, 17, 591–599, doi:http://dx.doi.org/10.1175/JHM-D-15-0096.1.
- 679 Han, S., Kim, H., Yeo, I., Yeh, I., Oki, T., Seo., K., Alsdorf, D. and Luthcke, S. B. (2009). Dy-  
680 namics of surface water storage in the Amazon inferred from measurements of inter-satellite  
681 distance change. *Geophysical Research Letters*, 36(9), doi:10.1029/2009GL037910.
- 682 Haohan, W., Xiufeng, H. and Zheng, J. (2013). Terrestrial water storage variations in Southwest  
683 China revealed by gravity mission and hydrologic and climate model. *Journal of Natural*  
684 *Sciences*, 41(6), 488–492.
- 685 Harter, T. (2001). Groundwater Hydrology. *California Department of Water Resources*, pp. 1-  
686 2. Accessed from <http://groundwater.ucdavis.edu/files/136254.pdf> on September 9,  
687 2016.
- 688 Hirata, R., Conicelli, B. P. (2012). Groundwater resources in Brazil: a review of possible im-  
689 pacts caused by climate change. *Anais da Academia Brasileira de Ciencias*, 84(2), 297–312,  
690 doi:http://dx.doi.org/10.1590/S0001-37652012005000037.
- 691 Hualan, R. and Hiroko, B. (2016). Global Land Data Assimilation System Version 2 (GLDAS-  
692 2) Products. Accessed from [http://hydro1.sci.gsfc.nasa.gov/data/s4pa/GLDAS/GLDAS\\_](http://hydro1.sci.gsfc.nasa.gov/data/s4pa/GLDAS/GLDAS_NOAH10_M.2.0/doc/README_GLDAS2.pdf)  
693 [NOAH10\\_M.2.0/doc/README\\_GLDAS2.pdf](http://hydro1.sci.gsfc.nasa.gov/data/s4pa/GLDAS/GLDAS_NOAH10_M.2.0/doc/README_GLDAS2.pdf) on September 22, 2016.
- 694 Huffman, G. J. and Bolvin, D. (2015). Real-Time TRMM Multi-Satellite Precipitation Analy-  
695 sis Data Set Documentation. Access from: [https://pmm.nasa.gov/sites/default/files/](https://pmm.nasa.gov/sites/default/files/document_files/3B4XRT_doc_V7.pdf)  
696 [document\\_files/3B4XRT\\_doc\\_V7.pdf](https://pmm.nasa.gov/sites/default/files/document_files/3B4XRT_doc_V7.pdf) on September 22, 2016.
- 697 Jekeli, C. (1981). Alternative methods to smooth the Earth’s gravity field. *Technical Report*,  
698 Rep 327.
- 699 Kummerow, C., William, B., Toshiaki, K., James, S., and Simpson, J. (1998) The tropical  
700 rainfall measuring mission (TRMM) sensor package. *Atmos Oceanic Tech*, 809, 15–17.

- 701 Landerer, F. W., and Swenson, S. C. (2012). Accuracy of scaled GRACE terrestrial water  
702 storage estimates. *Water Resources Research*, 48, W045531, doi:10.1029/2011WR011453.
- 703 Lemos, M. C., Finan, T. J., Fox, R. W., Nelson, D. R. and Tucker, J. (2002). The use of seasonal  
704 climate forecasting in policymaking: Lessons from northeast Brazil. *Climatic Change*, 55(4),  
705 479–597, doi:10.1023/A:1020785826029.
- 706 Marengo, J. A., Torres, R. R. and Alves, L. M. (2016). Drought in Northeast Brazilpast, present,  
707 and future. *Theoretical and Applied Climatology*, pp. 1-12, doi:10.1007/s00704-016-1840-8.
- 708 Marimon, M. P. C., Roisenberg, A., Suhogusoff, A. V. &Viero, A. P. (2013). Hydrogeo-  
709 chemistry and statistical analysis applied to understand fluoride provenance in the guarani  
710 aquifer system, southern Brazil. *Environmental Geochemistry and Health*, 35(3), 391–403,  
711 doi:10.1007/s10653-012-9502-y.
- 712 Melo, D., Scanlon, B. R., Zhang, Z. and Wendland, E. (2016). Reservoir storage and hydrologic  
713 responses to droughts in the Paran River Basin, Southeast Brazil. *Hydrol. Earth Syst. Sci.*  
714 *Discuss*, doi:10.5194/hess-2016-258.
- 715 Mendonça, L. A., Ribeiro, Frischkorn, H., Santiago, M. F. and Filho, J. M. (2005). Isotope  
716 measurements and groundwater flow modeling using MODFLOW for understanding envi-  
717 ronmental changes caused by a well field in semiarid Brazil. *Environmental Geology*, 47(8),  
718 1045–1053, doi:10.1007/s00254-005-1237-y.
- 719 Müller Schmeid, H., Eisner, S., Franz, D., Wattenbach, M., Portmann, F. T., Flörke, M. and  
720 Döll, P. (2014). Sensitivity of simulated global-scale freshwater fluxes and storages to input  
721 data, hydrological model structure, human water use and calibration. *Hydrology and Earth*  
722 *System science*, 18, 3511–3538, doi:10.5194/hess-18-3511-2014.
- 723 Nanteza, J., de Linage, C. R., Thomas, B. F. and Famiglietti, J. S. Monitoring groundwater  
724 storage changes in complex basement aquifers: An evaluation of the GRACE satellites over  
725 East Africa. *Water Resource Research*, doi:10.1002/2016WR018846.
- 726 Negri, A. J., Adler, R. F., Xu, L. &Surratt, J. (2004). The impact of Amazonian deforestation  
727 on dry season rainfall. *Climate*, 17(6), 1306–1319.
- 728 Nelson, S. A. (2015). Groundwater. *Physical Geology, EENS*, 1100.



- 729 Norbre, C. A., Marengo, J. A., Seluchi, M. E., Cuartas, L. A., Alves, L. M. (2016).  
730 Some Characteristics and Impacts of the Drought and Water Crisis in Southeastern  
731 Brazil during 2014 and 2015. *Journal of Water Resource and Protection*, 8(2), 252–262,  
732 doi:10.4236/jwarp.2016.820.22.
- 733 Ondra, R. (2002). Geochemical and stable isotopic evolution of the Guarani Aquifer System in  
734 the state of São Paulo, Brazil. *Hydrogeology Journal*, 10, 643–655.
- 735 Otto, F. E. L., Coelho, C. A. S., King, A., ...Cullen, H. (2015). Factors other than climate  
736 changes, main drivers of 2014/15 water shortages in Southeast Brazil. *Bulletin of the Amer-*  
737 *ican Meteorological Society*, 96(12), S35–S40.
- 738 Paiva, R. C. D., Buarque, D. C., Collischonn, Bonnet, M. P., Frappart, F., Calmant, S. and  
739 Mendes, C. A. B. (2013). Large-scale hydrologic and hydrodynamic modeling of the Amazon  
740 River basin. *Water Resources Research*, 49, 1226–1243, doi:10.1002/wrcr.20067.
- 741 Pimentel, E. T. and Hamza, V. M. (2014). Use of geothermal methods in outlining deep ground-  
742 water flow systems in Paleozoic interior basins of Brazil. *Hydrogeology Journal*, 22, 107–128,  
743 doi:10.1007/s10040-013-1074-0.
- 744 Preisendorfer, R. W. (1988) Principal component analysis in meteorology and oceanography.  
745 *Elsevier*, New York.
- 746 Ricardo, H. and Bruno, P. C. (2011). Groundwater resources in Brazil: a review of possible  
747 impacts caused by climate change. *Annals of the Brazilian Academy of Sciences*, 84(2), 297–  
748 312, doi:10.1590/S0001-37652012005000037.
- 749 Rodell, M., Houser, P. R., Jambor, U., Gottschalck, J., et al. (2004) The global land data  
750 assimilation system. *Bull Am Meteorol Soc*, 85, 381–94, doi:10.1175/BAMS-85-3-381.
- 751 Rousseeuw, P. J., Ruts, I. and Tukey, J. W. (1999). The Bagplot: A Bivariate Boxplot. *The*  
752 *American Statistician*, 53(4), 382-387, doi:10.2307/2686061.
- 753 Rowland, L., Da Costa, A. C. L., Galbraith, D. R., ...Meir, P. (2015). Death from drought in  
754 tropical forests is triggered by hydraulics not carbon starvation. *Nature*, 528(7580), 119-122,  
755 doi:10.1038/nature15539.

- 756 Sawicz, K., Wagene, T., Sivapalan, M., Troch, P.A. and Carrillo, G. (2011). Catchment classification: empirical analysis of hydrologic similarity based on catchment function in the eastern  
757 USA. *Hydrology and Earth System Sciences*, 15, 2895–2911, doi:10.5194/hess-15-2895-2011.  
758
- 759 Sinha. D., Syed, T. H., Famiglietti, J. S., Reager, J. T. and Thomas, R. C. (2016). Characterizing Drought in India Using GRACE Observations of Terrestrial Water Storage Deficit.  
760 *Journal of Hydrometeorology*, doi:dx.doi.org/10.1175/JHM-D-16-0047.1.  
761
- 762 Soler, I. G. and Bonotto, D. M. (2015). Hydrochemical and stable isotopic (H,O,S) signatures  
763 in deep groundwaters of Parana basin, Brazil. *Environmental Earth Science*, 73(1),95–113,  
764 doi:10.1007/s12665-014-3397-0.
- 765 Swenson, S. and Wahr, J. (2006). Post-processing removal of correlated errors in GRACE data.  
766 *Geophysical Research Letters*, 33(8), L08402, doi:10.1029/2005GL025285.
- 767 Tapley, B. D., Bettadpur, S., Ries, J.C. et al. (2004). GRACE measurements of mass variability  
768 in the Earth system. *Science*, 305(5683), 503–505, doi:10.1126/science.1099192.
- 769 Tarpanelli, A., Barbetta, S., Brocca, L. and Moramarco, T. (2013). River Discharge Estimation  
770 by Using Altimetry Data and Simplified Flood Routing Modeling. *Remote Sensing*, 5, 4145–  
771 4162. doi:10.3390/rs5094145.
- 772 Tukey, J. W (1977). *Exploratory Data Analysis*. Addison-Wesley.
- 773 Vieceli, N., Bortolin, T. A., Mendes, L. A., Bacarim, G., Cemin, G. and Schneider, V. E. (2015).  
774 Morphometric evaluation of watersheds in caxias so sul city, Brazil, using SRTM(DEM) data  
775 and GIS. *Environmental Earth Science*, 73(9), 5677–5685, doi:10.1007/s12665-014-3823-3.
- 776 Wahr J, Molenaar M, Bryan F. (1998). Time variability of the Earth’s gravity field: Hydrolog-  
777 ical and oceanic effects and their possible detection using GRACE. *Journal of Geophysical*  
778 *Research*, 103(B12), 30205–30229.
- 779 Werth, S. and Guntner, A. (2010). Calibration analysis for water storage variability of the  
780 global hydrological model WGHM. *Hydrology and Earth system science*, 14, 59–78. Available  
781 at [www.hydrol-earth-syst-sci.net/14/59/2010/](http://www.hydrol-earth-syst-sci.net/14/59/2010/).
- 782 William, M. A. and Leonard, F. K. (2015) Bringing GRACE Down to Earth. *Groundwater*,  
783 53(6), 826–829, doi:10.1111/gwat.12379.

- 784 Xiao, R., He, X., Zhang, Y., Ferreira, V. G. & Chang, L. (2015). Monitoring Groundwater  
785 Variations from Satellite Gravimetry and Hydrological Models: A Comparison with in-situ  
786 Measurements in the Mid-Atlantic Region of the United States. *Remote Sensing*, 7, 686–703,  
787 doi:10.3390/rs70100686.
- 788 Zagonari, F. (2010). Sustainable, just, equal, and optimal groundwater management strategies  
789 to cope with climate change. Insights from Brazil. *Water Resources Management*, 24(13),  
790 3731–3756, doi:10.1007/s11269-010-9630-z.
- 791 Zheng, Q. Y. and Chen, S. (2015). Review on the recent developments of terrestrial water  
792 storage variations using GRACE satellite-based data. *Progress in Geophysics*, 30(6), 2603–  
793 2615, doi:10.6038/pg20150619.
- 794 Zhiyong, H., Yun, P., Huili, G., ... Wenji, Z. (2015). Subregional-scale groundwater depletion  
795 detected by GRACE for both shallow and deep aquifers in North China Plain. *Geophysical*  
796 *Research Letters*, 42(6), 1791–1799. doi:10.1002/2014GL06249.

**Supplementary material for on-line publication only**

**[Click here to download Supplementary material for on-line publication only: Supporting Material.pdf](#)**